HHS Public Access

Author manuscript

*Neuron*. Author manuscript; available in PMC 2024 June 05.

Published in final edited form as:

*Neuron*. 2023 April 05; 111(7): 1118–1135.e5. doi:10.1016/j.neuron.2022.12.034.

# Local 5-HT signaling bi-directionally regulates the coincidence time window for associative learning

**Jianzhi Zeng**[1,2,3,4,5,6,14,*], **Xuelin Li**[1,3,5,14], **Renzimo Zhang**[1,3,4,5,7], **Mingyue Lv**[1,3,5], **Yipan Wang**[1,3,5], **Ke Tan**[1,3], **Xiju Xia**[1,3,5,8], **Jinxia Wan**[1,3,5], **Miao Jing**[9], **Xiuning Zhang**[1,3,5], **Yu Li**[10], **Yang Yang**[11,12], **Liang Wang**[13], **Jun Chu**[13], **Yan Li**[11,12], **Yulong Li**[1,2,3,4,5,7,8,9,15,*]

[1]State Key Laboratory of Membrane Biology, School of Life Sciences, Peking University, Beijing 100871, China

[2]Institute of Molecular Physiology, Shenzhen Bay Laboratory, Shenzhen 518132, China

[3]PKU-IDG/McGovern Institute for Brain Research, Beijing 100871, China

[4]Peking-Tsinghua Center for Life Sciences, Academy for Advanced Interdisciplinary Studies, Peking University, Beijing 100871, China

[5]National Biomedical Imaging Center, Peking University, Beijing 100871, China

[6]Hefei National Laboratory for Physical Sciences at the Microscale, CAS Key Laboratory of Brain Function and Disease, School of Life Sciences, Division of Life Sciences and Medicine, University of Science and Technology of China, Hefei 230026, Anhui, China

[7]Yuanpei College, Peking University, Beijing 100871, China

[8]PKU-THU-NIBS Joint Graduate Program, Beijing 100871, China

[9]Chinese Institute for Brain Research, Beijing 102206, China

[10]School of Medicine, The Chinese University of Hong Kong, Shenzhen 518172, China

[11]Institute of Biophysics, State Key Laboratory of Brain and Cognitive Science, Center for Excellence in Biomacromolecules, Chinese Academy of Sciences, Beijing 100101, China

[12]University of Chinese Academy of Sciences, Beijing 100049, China

[*]Correspondence: zengjz@szbl.ac.cn (J.Z.), yulongli@pku.edu.cn (Y.L.).

AUTHOR CONTRIBUTIONS

Yulong Li supervised the project. J.Z. and X.L. performed all functional imaging experiments (except as otherwise noted) and the immunofluorescence imaging. R.Z. and X.L. performed the behavioral experiments. R.Z. and X.L. analyzed the transcriptomics and EM data. M.L. contributed Figures S4D–S4F and S6A–S6C. R.Z., Y.W., and K.T. contributed Figures 4A–4C and S4A–S4C. K.T. and Y.W. contributed data to Figures S1A–S1C. X.X. contributed Figures S6D–S6G. X.L., X.Z., and M.L. contributed Figure 6. Yu Li contributed Figure 5C. Y.Y. and Yan Li helped to construct the setup for Figures 3A–3F. J.W. and M.J. provided the 5-HT1.0 and ACh3.0 sensors, respectively. L.W. and J.C. provided the G-Flamp1 sensor. All authors contributed to the data analysis. Yulong Li, J.Z., and X.L. wrote the manuscript with input from all other authors.

SUPPLEMENTAL INFORMATION

Supplemental information can be found online at https://doi.org/10.1016/j.neuron.2022.12.034.

DECLARATION OF INTERESTS

The authors declare no competing interests.

[13]Guangdong Provincial Key Laboratory of Biomedical Optical Imaging Technology & Center for Biomedical Optics and Molecular Imaging & CAS Key Laboratory of Health Informatics, Shenzhen Institute of Advanced Technology, Chinese Academy of Sciences, Shenzhen 518055, China

[14]These authors contributed equally

[15]Lead contact

## SUMMARY

The coincidence between conditioned stimulus (CS) and unconditioned stimulus (US) is essential for associative learning; however, the mechanism regulating the duration of this temporal window remains unclear. Here, we found that serotonin (5-HT) bi-directionally regulates the coincidence time window of olfactory learning in *Drosophila* and affects synaptic plasticity of Kenyon cells (KCs) in the mushroom body (MB). Utilizing GPCR-activation-based (GRAB) neurotransmitter sensors, we found that KC-released acetylcholine (ACh) activates a serotonergic dorsal paired medial (DPM) neuron, which in turn provides inhibitory feedback to KCs. Physiological stimuli induce spatially heterogeneous 5-HT signals, which proportionally gate the intrinsic coincidence time windows of different MB compartments. Artificially reducing or increasing the DPM neuron-released 5-HT shortens or prolongs the coincidence window, respectively. In a sequential trace conditioning paradigm, this serotonergic neuromodulation helps to bridge the CS-US temporal gap. Altogether, we report a model circuitry for perceiving the temporal coincidence and determining the causal relationship between environmental events.

## Graphical abstract

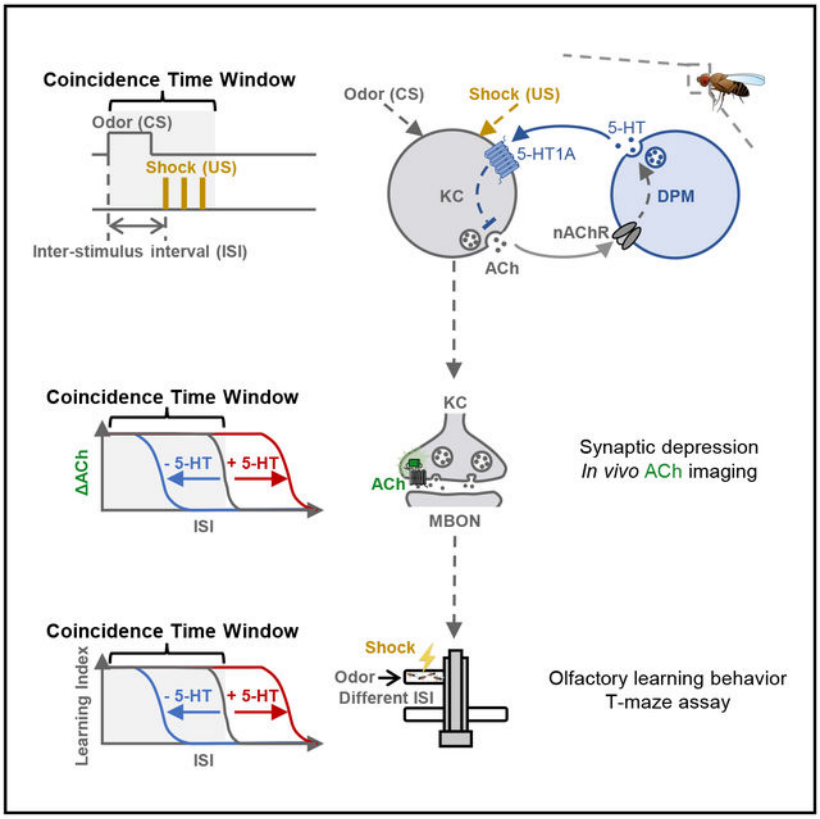


## In brief

The coincidence time window is the maximal temporal interval that allows two stimuli to be associated in Pavlovian learning. However, its neuronal mechanism remains unclear. Zeng et al. identify a serotonergic circuitry that regulates the coincidence time window for Drosophila olfactory learning, shedding light on the mystery left by Ivan Pavlov.

## INTRODUCTION

To survive in the constantly changing environment, animals have evolved associative learning to build a causal relationship between a neutral conditioned stimulus (CS) and the subsequent punitive or rewarding unconditioned stimulus (US). A prerequisite for successfully building the association in Pavlovian conditioning[1] is that the inter-stimulus interval (ISI) of the CS and US must fall within a relatively brief coincidence time window. This temporal coincidence exists in a wide range of species, including in the eye-blinking task in humans,[2,3] the siphon withdrawal reflex in *Aplysia*,[4,5] and olfactory or visual associative learning in flies and bees.[6–10] Importantly, shifted coincidence time windows have been reported in brain injuries and psychological diseases.[11–18] Thus, elucidating the mechanism of coincidence time window will provide valuable insights into how the brain estimates the relationship between two temporally discrete events and shed new light on how brain disorders affect associative learning.

*Drosophila* is a classical model organism for studying the mechanism of associative learning owing to the robustness of the olfactory learning paradigm and the genetic tractability of the olfactory learning center mushroom body (MB).[19–22] To elicit the aversive olfactory memory by pairing the odor (CS) with an electric shock (US), these two stimuli must follow a specific order (shock after odor) and arrive in the coincidence time window, which is on the order of tens of seconds.[6,10,23–26] It has been reported that dopamine (DA) receptors impose the input-order requirement with different downstream cascades.[27–30] However, the specific molecules and circuits that gate the length of the coincidence window remain unclear, even though numerous studies have attempted to tackle this mechanism by performing behavioral and functional imaging experiments.[31–33]

In the MB of each hemisphere, ~2,000 Kenyon cells (KCs) bundle their axons into three lobes, called the α/β, α′/β′, and γ lobes, and each lobe is further segmented into 5 compartments. The compartment serves as an anatomical and functional unit, where the projection neuron-mediated olfactory signal (CS) and the dopaminergic neuron (DAN)-mediated electric shock signal (US) converge on the KCs, and KCs release acetylcholine (ACh) to activate the MB output neurons (MBONs).[34–40] Besides DA and ACh, the MB microcircuit also orchestrates other neuromodulators to implement specialized functions of the intricate learning process, including octopamine (OA), γ-aminobutyric acid (GABA), glutamate, and 5-hydroxytryptamine (5-HT). There is only one serotonergic dorsal paired medial (DPM) neuron innervating three MB lobes, which is reported to be involved in olfactory learning.[41–55] Nevertheless, little is known regarding the *in vivo* dynamics of 5-HT release from the DPM neuron, as well as its upstream regulations and downstream functions.

Here, we show that the coincidence time windows of olfactory learning and the change of synaptic plasticity are coherently regulated by 5-HT released from the DPM neuron in *Drosophila*. Using GPCR-activation-based (GRAB) sensors for ACh and 5-HT ($GRAB_{ACh3.0}$ and $GRAB_{5\text{-}HT1.0}$, hereafter referred to as ACh3.0 and 5-HT1.0, respectively),[56–58] we observed compartmentally heterogeneous 5-HT release in response to odor and electric shock. We also identified the reciprocal connections between the DPM neuron and KCs, where the DPM neuron is activated by KCs and in turn provides inhibitory feedback to the KCs. This serotonergic DPM neuron-mediated feedback circuit shapes the intrinsic time windows of different MB compartments and improves the learning performance in a trace conditioning paradigm.

## RESULTS

### 5-HT regulates the coincidence time window of single-trial olfactory learning

To measure the coincidence time window of olfactory learning, we used the T-maze to train flies by pairing an odor (CS+) and the electric shock (US) with varying ISIs, while leaving another odor as the unpaired stimulus (CS−). Then we tested the flies' preference between CS+ and CS− and calculated the performance index (PI) of learning (Figures 1A and 1B). We found that control flies learned to avoid the CS+ only when the ISI was ≤ 15 s (Figure 1C). We applied a sigmoid function to the relationship between the relative PI and the ISI; the coincidence time window corresponds to the $t_{50}$ of the fitted curve, which was 16.9 s for control flies. We then examined the $Trhn^{-/-}$ flies,[59] which lack the rate-limiting tryptophan

hydroxylase neuronal (Trhn) in 5-HT biosynthesis, and found that the coincidence time window was shortened to 10.8 s (Figure 1D). Conversely, when we fed flies with the fluoxetine—a selective serotonin reuptake inhibitor (SSRI)—to increase the extracellular 5-HT level,[54,60] the coincidence time window was extended to 25.2 s (Figure 1E). Together, these results suggest that the 5-HT signal bi-directionally regulates the coincidence time window of olfactory learning.

## 5-HT regulates the coincidence time window of synaptic depression

One potential mechanism that explains the shift of the coincidence time window in olfactory learning is that 5-HT regulates the change in synaptic plasticity underlying memory formation. Previous electrophysiological recording and $Ca^{2+}$ imaging studies in the MBON innervating the γ1 compartment (MBON-γ1pedc) suggest that pairing an odor with dopaminergic reinforcement induces synaptic depression between KCs and the MBON.[61–63] Here, we trained the head-fixed fly under two-photon microscope with a similar protocol to our T-maze assay (Figures 2B and S1B), and we performed *in vivo* imaging with ACh3.0 expressed in KCs (Figure 2A) or the $Ca^{2+}$ probe GCaMP6s expressed in MBON- γ1pedc (Figure S1A). Comparing the odor-evoked responses pre- and post-pairing, we observed synaptic depression only for the CS+, but not for the CS− (Figures 2C and S1C), consistent with previous reports.

Studying the coincidence time window that allows synaptic depression to happen, we systematically examined the change of ACh release (ΔACh) after odor-shock pairing with different ISIs. In control flies, significant synaptic depression occurred only when the ISI was ≤ 14 s (Figures 2D and S2A), with a $t_{50}$ of 14.8 s, on par with the $t_{50}$ of 16.9 s measured for aversive learning with T-maze (Figure 1C). Next, we found that the coincidence time windows in $Trhn^{-/-}$ flies and SSRI-treated flies were shifted to 12.4 s (Figures 2E and S2B) and 18.0 s (Figures 2F and S2C), respectively. These results indicate that 5-HT bi-directionally regulates the coincidence time window for altering synaptic plasticity in the γ1 compartment.

## Physiological stimuli trigger heterogeneous 5-HT release from single DPM neuron

In each hemisphere, the neuropil of the single serotonergic DPM neuron ramifies throughout MB lobes (Figure S1D). Although previous studies report the physiological activity of the DPM neuron with GCaMP or synapto-pHluorin,[44] the 5-HT dynamics are still unknown owing to a lack of tools. The development of the serotonin GRAB sensor, i.e., 5-HT1.0, allows us to selectively detect 5-HT release from the DPM neuron through *in vivo* imaging. Optogenetic activation of the DPM neuron triggered homogeneous release of 5-HT in the γ1–γ5 compartments, in a pulse number-dependent manner (Figures 3A–3F). By contrast, the physiological stimuli, such as odor application and electric shock, induced compartmentally heterogeneous 5-HT release, and the 5-HT signals vanished when the DPM neuron was silenced by potassium channel Kir2.1, or the 5-HT synthesis was impeded by mutating the Trhn gene (Figures 3G–3I). These heterogeneous patterns were not due to unequal expression of 5-HT1.0 sensor along the KCs' axon, because externally applied 5-HT still elicited equivalent fluorescence increase (Figure 3J). These results prompted us

to further examine the regulation underlying these heterogeneous 5-HT signals and the functional role they play in regulating the coincidence time window.

## The DPM neuron and KCs are reciprocally connected and functionally correlated

We next explored the DPM neuron's upstream and downstream connections in the MB by analyzing recently published EM connectomics.[64–67] The results show that the DPM neuron forms reciprocal connections with most of the cell types within the MB microcircuit, among which KCs comprise more than 80% of the DPM neuron's upstream synapses and more than 50% of the DPM neuron's downstream synapses (Figures S3A–S3G). We examined a total of 1,931 KCs and found that each KC forms reciprocal connections with the DPM neuron.

To elucidate the functional relationship between the DPM neuron and KCs, we used the GCaMP5 and 5-HT1.0 to detect the activity of and 5-HT release from the DPM neuron, respectively, and adopted the ACh3.0 to measure ACh release from KCs (Figure S3H). Comparing the odor- and electric shock-evoked changes in fluorescence of γ2–γ5 compartments, we found that the $Ca^{2+}$ and 5-HT signals were directly correlated with the ACh signals (Figures S3I and S3J), suggesting that the DPM neuron and KCs are not only reciprocally connected but also functionally correlated.

## KCs are both necessary and sufficient for activating the DPM neuron

Determining the input-output relationship between the DPM neuron and KCs, we utilized the chemogenetic silencer $G_{\alpha i}$-coupled hM4Di-DREADD[68] to inactivate the KCs with deschloroclozapine (DCZ)[69] and found that odor- and shock-induced 5-HT signals in the γ lobe were abolished (Figures 4A–4C). Meanwhile, the DCZ application showed no significant effect on stimuli-induced 5-HT signals in flies without hM4Di (Figures S4A–S4C). These results suggest that the excitatory input from KCs is required to trigger 5-HT release from the DPM neuron in physiological conditions.

Next, we found that applying ACh—but not other neurotransmitters, i.e., DA, OA, glutamate, or GABA—was sufficient to induce 5-HT release in the horizontal lobe that includes the γ lobe, and this excitatory effect could be blocked by mecamylamine (Meca), a nicotinic ACh receptor (nAChR) antagonist (Figures S4D–S4F). Optogenetic activation of the KCs also caused the release of 5-HT in a pulse number-dependent manner (Figures S4G–S4I). However, the light-induced 5-HT release disappeared in transgenic flies with UAS-CsChrimson but without KC-Gal4, ruling out the unspecific effect due to the leaky expression of channelrhodopsin (Figures S4J–S4M).[70] Furthermore, we found that the light-induced response was compromised by Meca, but not by the muscarinic ACh receptor (mAChR) antagonist tiotropium (Tio) (Figures 4D–4F), which is consistent with the documented transcriptomic data[71] showing that nAChRs, instead of mAChRs, are enriched in the DPM neuron (Figure S3K). Finally, we found that two-photon laser-mediated local stimulation of KCs could readily evoke highly localized 5-HT release (Figures S4N–S4P). Thus, the activation of KCs is both necessary and sufficient to drive the release of 5-HT from the DPM neuron.

## The DPM neuron provides inhibitory feedback to KCs

Having shown the excitatory signaling from KCs to the DPM neuron, we next examined signaling in the opposite direction—from the DPM neuron to KCs. We optogenetically activated the DPM neuron and measured both tonic and physiological stimuli-induced phasic ACh dynamics in the γ lobe (Figure 4G). Given that the DPM neuron is reported to couple with the GABAergic anterior paired lateral (APL) neuron via gap junctions,[46] we applied gap junction blocker carbenoxolone (CBX) to avoid indirect activation.[72] We found that activating the DPM neuron significantly reduced both tonic and phasic ACh signals (Figures 4H–4K and S5A–S5E). As negative controls, these inhibitory effects were not observed, neither in flies only with UAS-CsChrimson but without DPM-Gal4 (Figures S5F–S5I) nor in $Trhn^{-/-}$ flies (Figures S5J–S5L). Analysis of transcriptomic data[71] suggests that 5-HT1A and 5-HT1B receptors—both of which are coupled to the inhibitory $G_{\alpha i}$ pathway[73]—are enriched in KCs of the γ lobe (Figure S3L). Here, we found that the DPM neuron-mediated inhibition of the tonic ACh level could be specifically blocked by the 5-HT1A receptor antagonist, WAY-100635,[74] but was not sensitive to 5-HT2A, 5-HT2B, and 5-HT1B receptor antagonists (Figures 4J and 4K). Although the DPM neuron has also been reported to co-release GABA,[50] functional imaging experiments suggested that $GABA_A$ or $GABA_B$ receptor antagonists did not influence the DPM neuron-mediated inhibition (Figures S6A–S6C). Moreover, analysis of transcriptomic data[71] revealed that the abundance of genetic markers for the GABAergic neuron is extremely low in the DPM neuron (Figure S3M). To examine whether the APL neuron would be influenced by optogenetically activating the DPM neuron, we probed the APL neuron's activity with GCaMP5 in the absence of CBX and found that the $Ca^{2+}$ signal was virtually unaffected during light stimulation, whereas it responded robustly to odor stimulation (Figures S6D–S6G).[75–78] In summary, the tonic and phasic ACh dynamics are suppressed by 5-HT from the DPM neuron.

Given that (1) 5-HT1A couples the inhibitory $G_{ai}$ pathway,[73] and (2) the classical model of olfactory learning centers on the adenylyl cyclase, rutabaga, which is believed to integrate the CS and US signals then elevate the cAMP level within KCs,[6,10,23,26,27,29,79–84] it is critical to explore the influence of activating the DPM neuron on both tonic and phasic cAMP signals (Figure 4L). Here, we adopted a recently published cAMP sensor, G-Flamp1,[85] and found that unlike the ACh signals, activating the DPM neuron did not affect the phasic cAMP increase but selectively turned down the tonic cAMP level via 5-HT1A (Figures 4M–4P and S6H–S6J).

Altogether, we dissected the reciprocal relationship between the DPM neuron and KCs in the γ lobe, in which KCs release ACh to locally activate the DPM neuron via nAChRs, and in turn the DPM neuron releases 5-HT to inhibit intracellular cAMP of and ACh release from KCs via the 5-HT1A receptor (Figure 5A).

## 5-HT dynamics gate the coincidence time windows of synaptic depression in different MB compartments

Having studied the coincidence time window of synaptic plasticity in the γ1 compartment by systematically changing the 5-HT level, we next wanted to test whether the coincidence time window would be modulated specifically by the 5-HT signaling from the DPM neuron

to KCs (Figures 5A and 5B). We first examined flies expressing Gal4 in the DPM neuron and measured a 14.2-s coincidence time window (Figures 5C and S2D), which is akin to the one of 14.8 s in control flies (Figure 2D). When the DPM neuron was silenced by Kir2.1 or optogenetically activated through CsChrimson, the coincidence time windows were shortened to 10.9 s or prolonged to 24.0 s, respectively (Figures 5D, 5E, S2E, and S2F). The prolonged effect of optogenetic activation relied on 5-HT synthesis, as it disappeared when combining with the genetic background of $Trhn^{-/-}$ (Figures 5F and S2G). The 5-HT signal perceived by KCs is critical for the maintenance of the coincidence time window, because it was shortened in 5-$HT1A^{-/-}$ flies and KC > 5-HT1A-RNAi flies to 12.0 and 13.0 s, respectively (Figures 5G, 5H, S2H, and S2I).

Given that heterogeneous 5-HT signals were observed upon physiological stimuli, we speculated that these patterns would endow MB compartments with intrinsically distinct lengths of the coincidence time window. To test this hypothesis, we first examined the changes in synaptic plasticity (ΔCh) in γ2–γ5 compartments after odor-shock pairing through ACh3.0 imaging (Figures 6A and 6B) and observed significant depression in the γ2 and γ3 compartments (Figure 6C),[86] which together with the γ1 compartment are known to mediate the approaching behavior.[87] By examining the ΔACh with different ISIs, we measured the coincidence time windows of 17.4 and 23.3 s for the γ2 and γ3 compartments (Figures 6D–6G), respectively, which were directly correlated with the physiological 5-HT dynamics (Figure 6H).

## 5-HT released from the DPM neuron serves as a specialized regulator of the coincidence time window in olfactory learning

In olfactory learning behavior, the coincidence time window could also be regulated by specifically manipulating the DPM neuron via the inhibitory Kir2.1 or the excitatory CsChrimson, as it was shortened or prolonged to 10.4 or 44.1 s, respectively, compared with the 16.1-s $t_{50}$ of the flies carrying DPM-Gal4 (Figures 7A–7E). In addition, the regulation depends on the 5-HT signal released from the DPM neuron and perceived by KCs, because the coincidence time window could be extended to 33.3 s by specifically overexpressing Trhn in the DPM neuron (Figure 7F) or shortened to 14.7 and 10.6 s in 5-$HT1A^{-/-}$ flies and KC > 5-HT1A-RNAi flies, respectively (Figures 7H and 7I). By contrast, the DPM > Gad1-RNAi flies, which lack glutamic acid decarboxylase 1 (Gad1) for GABA synthesis, exhibited a 17.0-s coincidence time window, suggesting that GABA signal from the DPM neuron is dispensable in this process (Figure 7G).[50]

When systematically analyzing all data obtained from flies with different genetic or pharmacological perturbations, we found that changing the serotonergic neuromodulation from the DPM neuron generally did not affect the amplitudes of PI or ΔACh with short ISIs (Figures 8A and S7A–S7J). Instead, the DPM neuron-released 5-HT plays a specialized role in coherently regulating the coincidence time windows at both circuitry and behavioral levels, resulting in a direct correlation of these two processes (Figures 8B and 8C). Specifically, activating the serotonergic neurotransmission from the DPM neuron to KCs—e.g., in SSRI-fed flies and DPM > CsChrimson flies with light stimulation—extends the

coincidence time window; conversely, inhibiting the DPM-to-KCs signaling—e.g., in Trhn$^{-/-}$ flies, DPM > Kir2.1 flies, 5-HT1A$^{-/-}$ flies, and KC > 5-HT1A-RNAi flies—shortens the coincidence time window. In addition, we noticed interesting changes in the Hill coefficient of sigmoid function in different fly groups (Figures S7K and S7L), implying that 5-HT may interfere with a cooperative machinery within the KCs, which awaits to be addressed in the future.

### Serotonergic neuromodulation of the DPM neuron helps to bridge the temporal gap between CS and US

Our findings prompted us to investigate in which functional context the DPM-mediated serotonergic neuromodulation may apply. Given that a 10-s odor was used in our experiments, and all the measured coincidence time windows were ≥10 s, the DPM-released 5-HT seems to specifically regulate trace conditioning (with temporally separated CS and US) but not delay conditioning (with overlapped CS and US). Therefore, we focused on a sequential trace conditioning paradigm,[7,31] in which insects trained with ascending ISIs (from 15 to 35 s) exhibit better learning performance than the ones trained with descending ISIs (from 35 to 15 s). Utilizing a similar paradigm (Figures S8A and S8B), we found that the improved performance in the ascending group was only observed in control flies—not in DPM > Kir2.1 flies or Trhn$^{-/-}$ flies (Figure S8C)—suggesting that the DPM neuron and 5-HT contribute to bridging the temporal gap between CS and US during ascending pairing.

To examine the changes in synaptic plasticity, we performed live imaging with ACh3.0 in the $\gamma$1 compartment (Figures S8D and S8E). The ACh signals in response to CS+ were depressed in the ascending group (Figure S8F) but were not changed in the descending group (Figure S8G), which conformed with the difference in behavior. Interestingly, in the descending group, the ACh release triggered by CS− was further potentiated, which explained why olfactory learning still existed. A similar synaptic potentiation associated with CS− has also been reported previously, which involves the reconsolidation of olfactory memory.[88]

To elucidate the role of 5-HT, we examined its dynamics throughout these trace conditioning paradigms and found significant potentiation in response to CS+ in three pairing trials (i.e., at ISIs of 15, 20, and 25 s) in the ascending group (Figure S8H); by contrast, the potentiation was only observed in the first pairing trial (i.e., at an ISI of 35 s) in the descending group (Figure S8I). These results suggest that 5-HT release is experience dependent. In the ascending group, previous trials with brief ISIs potentiated the 5-HT release in subsequent trials; the increased and prolonged 5-HT signal expanded the coincidence time window, thereby helping to bridge the temporal gap between the CS and US.

## DISCUSSION

A century ago, Ivan Pavlov proposed the associative conditioning theory, stating as follows: “A… most essential requisite for … a new conditioned reflex lies in a coincidence in time of … the neutral stimulus with … the unconditioned stimulus.”[1] However, the molecular and circuitry underpinnings that guarantee the maintenance of the coincidence time window have been unknown since then. Here, we report that the coincidence time window of olfactory

learning in *Drosophila* is bi-directionally regulated by the 5-HT signal from the single DPM neuron, which forms a feedback inhibitory circuit with the KCs in the MB.

In a natural environment, flies do not experience the precisely controlled conditioned and unconditioned stimuli that we can deliver in a laboratory setting; as a consequence, their learning must be capable of adapting to changing CS/US regimens. Thus, the modulation due to 5-HT signaling improves their ability to successfully extract meaningful cause and effect. Additionally, studies have shown that the DPM neuron is involved in stress,[53,54] sociality,[89,90] and aging.[51,52] Therefore, we speculate that flies in different brain states shall accordingly exhibit different coincidence time windows due to the changes of serotonergic tone within the MB.

### Versatile functions of 5-HT signals in olfactory learning

Previously, the DPM neuron was reported to be required specifically during memory consolidation of 3-h middle-term memory after delay conditioning.[43,44,49] Here, we found that the DPM neuron plays a different role in trace conditioning, regulating the coincidence time window during memory formation. Interestingly, people also found that DA has different functions in delay conditioning and trace conditioning of visual learning via distinct receptors.[9] Another recent finding suggests that the DPM neuron also functions as a bridge between two groups of KCs—encoding visual and olfactory signals, respectively—to improve cross-modal learning.[91] Besides the DPM neuron, there is a serotonergic projection neuron (SPN) innervating DANs in the peduncle of the MB, which gates the formation of long-term memory.[92] Taken together, the 5-HT signals play versatile functions in different computational processes of olfactory learning.

### The intracellular cAMP signal and the regulation of coincidence time window

The adenylyl cyclase, rutabaga, and its product, cAMP, have been widely recognized as the key nodes in KCs for olfactory learning, but the regulation of the cAMP signal has not been fully explored. By directly imaging cAMP dynamics with G-Flamp1, we found that activating the DPM neuron selectively suppressed the tonic level, while the phasic signal remained unchanged (Figures 4L–4P and S6H–S6J), indicating that the cAMP is tightly controlled by the endogenous 5-HT signal.

It also remains unclear how the cAMP-related signaling cascades affect the neurotransmission of KCs. Here, we found that artificial activation of the $G_{\alpha i}$ signaling via hM4Di could eliminate physiological stimuli-evoked ACh release (data not shown) and subsequent 5-HT release from the DPM neuron (Figures 4A–4C). By contrast, endogenous activation of the $G_{\alpha i}$ signaling via 5-HT1A—in response to the DPM neuron-released 5-HT—just turned down the phasic and tonic ACh dynamics (Figures 4G–4K and S5A–S5C). These results emphasize the nuance of upstream regulations and downstream functions of the cAMP signal.

These results drove us to ask how the 5-HT affects intracellular cAMP signaling and regulates the coincidence time window. From the perspective of KCs' ensemble, a computational model suggests that the difference in cAMP levels between odor-responsive KCs and non-responsive KCs determines learning efficiency.[93] During odor-shock pairing,

5-HT released from the DPM neuron broadly suppresses cAMP in both odor-responsive and non-responsive KCs; thus, 5-HT indeed increases the signal-to-noise ratio and improves learning efficiency. We hypothesize that this improvement might become more prominent at relatively long ISIs, and in such a way 5-HT extends the coincidence time window.

### 5-HT serves as an additional timing-regulating factor in the neo-Hebbian learning rule

Apart from *Drosophila*, 5-HT is involved in learning and memory in a wide range of species, including *Aplysia*,[94,95] *C. elegans*,[96] and mammals.[97–100] A growing body of evidence supports the notion that 5-HT affects timing during reinforcement learning.[101–107] Human studies in a trace conditioning paradigm showed that decreasing 5-HT level by tryptophan deprivation specifically impaired learning with a long ISI.[108] By contrast, studies of the nictitating membrane response in rabbits found that the hallucinogenic lysergic acid diethylamide (LSD, a non-selective 5-HT receptor agonist) facilitates learning with a long ISI.[16,17] These findings are reminiscent of our observations in *Drosophila* in which 5-HT bi-directionally regulates the coincidence time window. Thus, a similar serotonergic mechanism may be recruited by both vertebrates and invertebrates.

The classic model of Hebbian plasticity suggests that co-activation of presynaptic and postsynaptic neurons within a short time window enables changes in synaptic plasticity, a phenomenon known as spike timing-dependent plasticity (STDP). Due to the inability of STDP to adequately explain reinforcement learning with a temporal gap, this theoretical framework was updated in the past decade by introducing a third factor encoded by the phasic activity of neuromodulators, mediating reinforcement, surprise, or novelty.[109–114] In this updated three-factor neo-Hebbian learning rule,[115] “co-activation” plants a flag at the synapse called an eligibility trace, which waits for the third factor to implement the change in synaptic strength and determine the direction of that change (i.e., synaptic depression vs. potentiation). The neo-Hebbian learning rule is also applied in the MB of arthropods, where STDP exits between KCs and MBONs,[116] with the dopaminergic reinforcement corresponding to the third factor. However, to the best of our knowledge, a putative fourth factor that specifically regulates the length of the eligibility trace remains unknown. Several theories have been proposed suggesting that 5-HT may serve as a timing regulator in a variety of processes, including reinforcement learning.[117,118] Consistent with these predictions, we here experimentally show that 5-HT signaling from the DPM neuron proportionally gates the coincidence time window, therefore serving as a specific timing-regulating factor that provides the missing piece of the puzzle.

## STAR★METHODS

### RESOURCE AVAILABILITY

**Lead contact—**Further information and requests for resources and reagents should be directed to and will be fulfilled by the lead contact, Yulong Li (yulongli@pku.edu.cn).

**Materials availability—**This study did not generate new unique reagents.

### Data and code availability

- All imaging data reported in this paper will be shared by the lead contact upon request.
- This paper does not report original code.
- Any additional information required to reanalyze the data reported in this paper is available from the lead contact upon request.

## EXPERIMENTAL MODEL AND SUBJECT DETAILS

### Fly strains

**Fly husbandry:** Flies were raised on corn meal at 25°C in 50% humidity, under a 12-hour light /12-hour dark cycle. For optogenetics, flies were transferred to corn meal containing 400 μM all-trans-retinal after eclosion and raised in the dark for 8–24 hours before imaging or behavioral experiments. For fluoxetine treatment, flies were transferred to a tube containing a filter paper loaded with 150 μl 5% (w/v) sucrose solution containing 10 mM fluoxetine for 14–20 hours before imaging or behavioral experiments.

**Detailed fly genotypes used by figures:** Figure 1. 1C, 1E: Canton-S (Control)

1D: Trh01 / Trh01 ($Trhn^{-/-}$)

Figure 2. 2A, 2C, 2D and 2F: LexAop2-ACh3.0 / CyO; MB247-LexA / TM6B

2E: R13F02-LexA / LexAop2-ACh3.0; Trh01 / Trh01

Figure 3. 3A–3F: UAS-CsChrimson-mCherry / R13F02-LexA; VT064246-Gal4 / LexAop2-5-HT1.0

3G–3J: UAS-5-HT1.0 / CyO; R13F02-Gal4 / TM2 (Control)

3G–3J: UAS-Kir2.1 / R13F02-LexA; VT064246-Gal4 / LexAop2-5-HT1.0 (DPM > Kir2.1)

3G–3J: R13F02-LexA / LexAop2-5-HT1.0; Trh01 / Trh01 ($Trhn^{-/-}$)

Figure 4. 4A–4C: UAS-hM4Di / +; UAS-5-HT1.0 / +; R13F02-Gal4 / +

4D–4F: UAS-CsChrimson-mCherry / R13F02-LexA; 30y-Gal4 / LexAop2-5-HT1.0

4G–4K: LexAop2-ACh3.0 / UAS-CsChrimson-mCherry; MB247-LexA / VT064246-Gal4

4L–4P: LexAop2-G-Flamp1 / UAS-CsChrimson-mCherry; MB247-LexA / VT064246-Gal4

Figure 5. 5C: LexAop2-ACh3.0 / +; VT064246-Gal4 / MB247-LexA

5D: LexAop2-ACh3.0 / UAS-Kir2.1; VT064246-Gal4 / MB247-LexA

5E: LexAop2-ACh3.0 / UAS-CsChrimson-mCherry; VT064246-Gal4 / MB247-LexA

5F: LexAop2-ACh3.0 / UAS-CsChrimson-mCherry; VT064246-Gal4,Trh01 / MB247-LexA,Trh01

5G: $5HT1A^{Gal4}$ / $5HT1A^{Gal4}$; MB247-LexA / LexAop2-ACh3.0

5H: LexAop2-ACh3.0 / +; MB247-LexA, 30y-Gal4 / UAS-5-HT1A-RNAi

Figure 6. 6A–6H: LexAop2-ACh3.0 / CyO; MB247-LexA / TM6B

Figure 7. 7C: VT064246-Gal4 / VT064246-Gal4

7D: UAS-Kir2.1 / CyO; VT064246-Gal4 / TM3

7E: UAS-CsChrimson-mCherry / CyO; VT064246-Gal4 / TM6B

7F: UAS-Trhn / UAS-Trhn; VT064246-Gal4,Trh01 / VT064246-Gal4,Trh01

7G: UAS-Gad1-RNAi / VT064246-Gal4

7H: $5HT1A^{Gal4}$ / $5HT1A^{Gal4}$

7I: UAS-5-HT1A-RNAi / 30y-Gal4

Figure S1. S1A–S1C: R12G04-lexA / CyO; LexAop2-GCaMP6s / TM2

S1D: UAS-CsChrimson-mCherry / R13F02-LexA; VT064246-Gal4 / LexAop2-5-HT1.0

Figure S3. S3H–S3J: LexAop2-ACh3.0 / CyO; MB247-LexA / TM6B (KC > ACh3.0)

S3H–S3J: UAS-GCaMP5 / CyO; VT064246-Gal4 / TM6B (DPM > GCaMP5)

S3H–S3J: UAS-5-HT1.0 / CyO; C316-Gal4 / TM2 (DPM > 5-HT1.0)

Figure S4. S4A–S4F: UAS-5-HT1.0 / CyO; R13F02-Gal4 / TM2

S4G–S4I, N-P: UAS-CsChrimson-mCherry / R13F02-LexA; 30y-Gal4 / LexAop2-5-HT1.0

S4J–S4M: UAS-CsChrimson-mCherry / R13F02-LexA; LexAop2-5-HT1.0 / + (without KC-Gal4)

S4J–S4M: UAS-CsChrimson-mCherry / R13F02-LexA; LexAop2-5-HT1.0 / 30y-Gal4 (with KC-Gal4)

Figure S5. S5A–S5E: LexAop2-ACh3.0 / UAS-CsChrimson-mCherry; MB247-LexA / VT064246-Gal4

S5F–S5I: LexAop2-ACh3.0 / UAS-CsChrimson-mCherry; MB247-LexA / + (without DPM-Gal4)

S5F–S5I: LexAop2-ACh3.0 / UAS-CsChrimson-mCherry; MB247-LexA / VT064246-Gal4 (with DPM-Gal4)

S5J–S5L: LexAop2-ACh3.0 / UAS-CsChrimson-mCherry; MB247-LexA,Trh01 / VT064246-Gal4,Trh01

Figure S6. S6A–S6C: LexAop2-ACh3.0 / UAS-CsChrimson-mCherry; MB247-LexA / VT064246-Gal4

S6D–S6G: L0111-lexA / GH146-Gal4; LexAop2-CsChrimson.tdTomato / UAS-GCaMP5

S6H–S6J: LexAop2-G-Flamp1 / UAS-CsChrimson-mCherry; MB247-LexA / VT064246-Gal4

Figure S8. S8A–S8C: Canton-S (Control)

S8A–S8C: Trh01 / Trh01 ($Trhn^{-/-}$)

S8A–S8C: UAS-Kir2.1 / CyO; VT064246-Gal4 / TM3 (DPM > Kir2.1)

S8F–S8G: LexAop2-ACh3.0 / CyO; MB247-LexA / TM6B

S8H–S8I: UAS-5-HT1.0 / CyO; R13F02-Gal4 / TM2

## METHOD DETAILS

**Behavioral experiments—**Experiments were conducted in a dark room at 22°C in 50–60% humidity. Flies within 24–72 hours after eclosion were transferred to a new tube 12 hours before the experiment. To avoid anesthesia during sorting, both female and male flies were used. A total of 50–100 flies were used for each trial. The odorants were diluted in mineral oil, with 3-octanol (OCT) and 4-methylcyclohexanol (MCH) diluted to 1:67 and 1:100, respectively. A flow of air was bubbled in the odorant-containing mineral oil and delivered to the training and testing arms of the T-maze at 800 ml/min. Before training, flies were accommodated in the training arm for 2 min.

For single-trial training shown in Figures 1 and 7, the CS+ was delivered via the airflow for 10 s. Electric shocks (US) were delivered (90 V, 1.25 s/pulse, 3 pulses at 0.2 Hz) via the copper grid contained within the training arm with varying ISIs. For optogenetic stimulation in Figure 7E, the light was delivered from the distal end of the training arm of T-maze, and the power was at 500~1500 $\mu W/mm^2$. 2 min after the end of the shocks, the CS- was delivered via the airflow for 10 s.

For five-trial training shown in Figures S8A–S8C, each trial contains the CS+ (10 s) paired with electric shocks (90 V, 1.25 s/pulse, 4 pulses at 0.2 Hz), and the CS− (10 s) being delivered 60 s after the end of the shocks. Between each trial, there was a 90-s break 1 min after training, the flies were transferred to the elevator and allowed to accommodate for 3 min before testing. During testing, the CS+ and CS− were delivered from two distal ends of the arms for 30 s, during which the flies were allowed to move freely to make their choice. The PI of one experiment was calculated as the difference in the number of flies in each arm divided by the sum of flies in both arms. The official PI was calculated as the average of two experiments with interchanged CS+ and CS− The deliveries of different stimuli, i.e., odors, shock and 635-nm light, were synchronized by Arduino.

***In vivo* imaging with two-photon microscope—**Adult female flies within 2 weeks after eclosion were used for the imaging experiments. Each fly was mounted to a customized chamber using tape, and a 1 mm × 1 mm rectangular section of tape above the head was removed. The cuticle between the eyes, air sacs, and fat bodies were sequentially and carefully removed in order to expose the brain. During dissection and the imaging experiments, the brain was bathed in adult hemolymph-like solution (AHLS) containing (in mM): 108 NaCl, 5 KCl, 5 HEPES, 5 D-trehalose, 5 sucrose, 26 $NaHCO_3$, 1 $NaH_2PO_4$, 2 $CaCl_2$ and 2 $MgCl_2$.

The functional imaging experiments were conducted using an Olympus FVMPE-RS microscope equipped with a Spectra-Physics InSight X3 dual-output laser. GFP-containing probes (including ACh3.0, 5-HT1.0, DA2m, GCaMP6s, GCaMP5 and G-Flamp1) were excited by a 920-nm laser and the signals were collected using a 495–540-nm filter. RFP-containing probes (mCherry and tdTomato) were excited by a 1045-nm laser and the signals were collected using a 575–630-nm filter. The 1045-nm excitation laser was also used for the two-photon optogenetic stimulation shown in Figures S4N–S4P and was delivered to the region of interest at ~ 20 mW.

For single-photon optogenetic stimulation, a 635-nm laser (Changchun Liangli Photo Electricity Co., Ltd.) was used, and the light was delivered to the brain via an optic fiber at ~ 180 μW/$mm^2$ in Figures 4D–4P, 5E, S4G–S4I, S5A–S5E, S5J–S5L, and S6, and at indicated powers in Figures S4J–S4M and S5F–S5I.

For odor stimulation, the odorant was first diluted by 200-fold (v/v) in mineral oil. An airflow was bubbled through the mineral oil at 200 ml/min, which was then converged with another pure airflow delivered at 800 ml/min. The combined airflow was finally delivered to the fly antenna at 1000 ml/min. For the experiments in Figures 3H, 4A–4C, S3H–S3J, and S4A–S4C, isoamyl acetate (IA) was used. For the experiments in Figures 2, 4G–4I, 4L–4N, 5, 6, S1A–S1C,S5A, S5B, S5D, S5E, S5J–S5L, S6D–S6G, S6H, S6I, and S8F–S8I, OCT and MCH were used. For all odor-shock pairing experiments, OCT and MCH was randomly selected as the CS+, with the other odorant being the CS−.

For electric shock stimulation, two copper wires were attached to the fly’s abdomen, and the voltage was set to 90 V.

The deliveries of different stimuli, i.e., odors, shock and 635-nm light, were synchronized by Arduino.

For the experiments in Figures 4J, 4K, 4O, 4P, S4D–S4F, S5C, S6A–S6C, and S6J, a small section of the blood-brain-barrier was carefully removed with tweezers before applying the indicated neurotransmitters and/or compounds.

**Immunostaining and confocal imaging—**The brains of female adult flies (7–14 days after eclosion) were dissected in ice-cold phosphate-buffered saline (PBS), fixed in ice-cold 4% (w/v) paraformaldehyde solution for 1 h, and washed 33× 10 min with washing buffer (PBS containing 3% NaCl and 1% Triton X-100). The brains were next incubated in penetration/blocking buffer (PBS containing 2% Triton X-100 and 10% normal goat serum)

for 20 h at 4°C on a shaker. The brains were then incubated with primary antibodies (diluted in PBS containing 0.25% Triton X-100 and 1% normal goat serum) for 24 hours at 4°C, and washed 33× 10 min in washing buffer on a shaker. The brains were incubated with the appropriate secondary antibodies (diluted in PBS containing 0.25% Triton X-100 and 1% normal goat serum) overnight at 4°C in the dark, and washed 33× 10 min with washing buffer on a shaker. The samples were finally mounted with Fluoroshield and kept in the dark. The following antibodies were used at the indicated dilutions: chicken anti-GFP (1:500), rabbit anti-mCherry (1:500), mouse anti-nc82 (1:40), Alexa Fluor 488 goat anti-chicken (1:500), Alex Fluor 555 goat anti-rabbit (1:500), and Alex Fluor 647 goat anti-mouse (1:500). Fluorescence images were obtained using a Nikon Ti-E A1 confocal microscope. Alexa Fluor 488, Alexa Fluor 555, and Alexa Fluor 647 were excited using a 485-nm, 559-nm, and 638-nm laser, respectively, and collected using a 525/50-nm, 595/50-nm, and 700/75-nm filter, respectively.

## QUANTIFICATION AND STATISTICAL ANALYSIS

All summary data are presented as the mean ± SEM, superimposed with individual data. The sample size for each experiment is indicated in the corresponding figure legend.

**Behavioral experiments—**The PI of one experiment was calculated using the following equation: $PI_{one\ exp} = [(N_{Cs-} - N_{CS+})/(N_{CS-} + N_{CS+})]$. If all flies failed to learn, PI = 0; if all flies avoided the shock-associated odor, PI = 1. To reduce the possible bias of innate preference, the official PI was the average of two experiments (one with OCT being the CS+, while another one with MCH being the CS+) calculated as follows: $PI = [(PI_{OCT\ CS+} + PI_{MCH\ CS+}) /2]$.

For the relative PI-ISI profiles shown in Figures 1 and 7, we defined $PI_{max}$ as the average of two PIs on the left (two short ISI data points; e.g., ISI = 5 and 10 s), and $PI_{min}$ as the average of two PIs on the right (two long ISI data points; e.g., ISI = 20 and 50 s). Relative $PI = [(PI - PI_{min})/(PI_{max} - PI_{min})]$. Error bars represent the $[(SEM\ of\ PI)/(PI_{max} - PI_{min})]$. The data were fitted with a sigmoid curve using the “DoseResp” function in Origin (OriginLab), resulting in a $t_{50}$ ± the standard error, Hill coefficient, and $R^2$.

***In vivo* imaging with two-photon microscope—**Images were processed using ImageJ software (National Institutes of Health). When generating the pseudocolor images, signals outside of the region of interest (outlined with white dashed lines) are eliminated to avoid distraction. The fluorescence response was calculated using the following equation: $\Delta F/F0 = [(F - F0) /F0]$, in which F0 is baseline fluorescence. The area under the curve was calculated using the integral of the fluorescence response ($\int \Delta F/F0$). In Figures 2, 5, 6, S1A–S1C, and S8F–S8G, the fluorescence responses measured during the 10-s odor application were included in $\int \Delta F/F0$. In Figures S8H and S8I, the fluorescence responses measured during the odor and shock application (65-s duration from the start of the odor application) were included in $\int \Delta F/F0$. Relative $\int \Delta F/F0$ was calculated by normalizing each $\int \Delta F/F0$ to the response measured during the corresponding pre-pairing session.

For each ΔACh-ISI profile shown in Figures 2, 5, and 6, $\Delta ACh = [(Relative \int \Delta F/F0_{pre}) - (Relative \int \Delta F/F0_{post})]$. The error bars represent the SEM of the relative ΔACh. The data

were fitted with a sigmoid curve using the “DoseResp” function in Origin (OriginLab), resulting in a $t_{50}$ ± the standard error, Hill coefficient, and $R^2$.

## Supplementary Material

Refer to Web version on PubMed Central for supplementary material.

## ACKNOWLEDGMENTS

We thank Yi Rao for providing access to the two-photon microscope. We thank Yi Zhong, Lianzhang Wang and Bohan Zhao for help with T-maze assay. We thank Liming Wang and Rui Huang for help in providing facilities of fly husbandry. We thank Yoshinori Aso for help in testing the optogenetic four-arm arena paradigm. We thank the imaging core facility of State Key Laboratory of Membrane Biology at Peking University (Ye Liang), Shenzhen Bay Laboratory (Zhenglong Sun, Mei Yu, and Shixian Huang), and Olympus/Evident China Life Science (Shaoling Qi, Wei Cao, Haitao Zhang, Dezhi Zhang, Linliang Yin, and Donghua Wu). We thank the Core Facility of *Drosophila* Resource and Technology of CAS Center for Excellence in Molecular Cell Science (Wei Wu). Finally, we thank Liqun Luo, Jing Wang, Quentin Gaudry, Scott Owen, Seth Tomchik, Ryohei Yasuda, Liang Liang, Ronald Davis, Li Liu, Yi Zhong, Jing Ren, Pu Fan, Stephen Zhang, Andrew Lutas, Bowen Deng, Fei Wang, Kaiyu Wang, and Yoshinori Aso for valuable feedback regarding the manuscript.

This research was supported by grants to Yulong Li from the National Key R&D Program of China (2019YFE011781), the National Natural Science Foundation of China (31925017), the NIH BRAIN Initiative (1U01NS113358 and 1U01NS120824), the Beijing Municipal Science & Technology Commission (Z220009), the Feng Foundation of Biomedical Research, the Clement and Xinxin Foundation, the Peking-Tsinghua Center for Life Sciences, and the State Key Laboratory of Membrane Biology at School of Life Sciences, Peking University; and by the grant to J.Z. from the China Postdoctoral Science Foundation.

## REFERENCES

1. Pavlov IP (1927). Conditioned Reflexes: an Investigation of the Physiological Activity of the Cerebral Cortex (Oxford University Press).
2. Bernstein AL (1934). Temporal factors in the formation of conditioned eyelid reactions in human subjects. J. Gen. Psychol 10, 173–197.
3. McAllister WR (1953). Eyelid conditioning as a function of the CS-US interval. J. Exp. Psychol 45, 417–422. 10.1037/h0059534. [PubMed: 13052882]
4. Hawkins RD, Carew TJ, and Kandel ER (1986). Effects of interstimulus interval and contingency on classical conditioning of the Aplysia siphon withdrawal reflex. J. Neurosci 6, 1695–1701. [PubMed: 3712005]
5. Carew TJ, Walters ET, and Kandel ER (1981). Classical conditioning in a simple withdrawal reflex in Aplysia californica. J. Neurosci 1, 1426–1437. [PubMed: 7320755]
6. Tully T, and Quinn WG (1985). Classical conditioning and retention in normal and mutant Drosophila melanogaster. J. Comp. Physiol. A 157, 263–277. [PubMed: 3939242]
7. Szyszka P, Demmler C, Oemisch M, Sommer L, Biergans S, Birnbach B, Silbering AF, and Galizia CG (2011). Mind the gap: olfactory trace conditioning in honeybees. J. Neurosci 31, 7229–7239. 10.1523/JNEUROSCI.6668-10.2011. [PubMed: 21593307]
8. Vogt K, Yarali A, and Tanimoto H (2015). Reversing stimulus timing in visual conditioning leads to memories with opposite valence in drosophila. PLoS One 10, e0139797. 10.1371/journal.pone.0139797. [PubMed: 26430885]
9. Grover D, Chen JY, Xie J, Li J, Changeux JP, and Greenspan RJ (2022). Differential mechanisms underlie trace and delay conditioning in Drosophila. Nature 603, 302–308. 10.1038/s41586-022-04433-6. [PubMed: 35173333]
10. Tanimoto H, Heisenberg M, and Gerber B (2004). Experimental psychology: event timing turns punishment to reward. Nature 430, 983. 10.1038/430983a.
11. Woodruff-Pak DS, and Papka M (1996). Huntington’s disease and eyeblink classical conditioning: normal learning but abnormal timing. J. Int. Neuropsychol. Soc 2, 323–334. 10.1017/s135561770000134x. [PubMed: 9375181]

12. McGlinchey-Berroth R, Brawn C, and Disterhoft JF (1999). Temporal discrimination learning in severe amnesic patients reveals an alteration in the timing of eyeblink conditioned responses. Behav. Neurosci 113, 10–18. 10.1037/0735-7044.113.1.10. [PubMed: 10197902]

13. Frings M, Gaertner K, Buderath P, Gerwig M, Christiansen H, Schoch B, Gizewski ER, Hebebrand J, and Timmann D (2010). Timing of conditioned eyeblink responses is impaired in children with attention-deficit/hyperactivity disorder. Exp. Brain Res 201, 167–176. 10.1007/s00221-009-2020-1. [PubMed: 19777220]

14. Oristaglio J, Hyman West S, Ghaffari M, Lech MS, Verma BR, Harvey JA, Welsh JP, and Malone RP (2013). Children with autism spectrum disorders show abnormal conditioned response timing on delay, but not trace, eyeblink conditioning. Neuroscience 248, 708–718. 10.1016/j.neuroscience.2013.06.007. [PubMed: 23769889]

15. Bolbecker AR, Steinmetz AB, Mehta CS, Forsyth JK, Klaunig MJ, Lazar EK, Steinmetz JE, O'Donnell BF, and Hetrick WP (2011). Exploration of cerebellar-dependent associative learning in schizophrenia: effects of varying and shifting interstimulus interval on eyeblink conditioning. Behav. Neurosci 125, 687–698. 10.1037/a0025150. [PubMed: 21942432]

16. Harvey JA (2003). Role of the serotonin 5-HT2A receptor in learning. Learn. Mem 10, 355–362. 10.1101/lm.60803. [PubMed: 14557608]

17. Harvey JA, Gormezano I, Cool-Hauser VA, and Schindler CW (1988). Effects of LSD on classical conditioning as a function of CSUCS interval: relationship to reflex facilitation. Pharmacol. Biochem. Behav 30, 433–441. 10.1016/0091-3057(88)90477-7. [PubMed: 3174776]

18. Perrett SP, Ruiz BP, and Mauk MD (1993). Cerebellar cortex lesions disrupt learning-dependent timing of conditioned eyelid responses. J. Neurosci 13, 1708–1718. [PubMed: 8463846]

19. Aso Y, Hattori D, Yu Y, Johnston RM, Iyer NA, Ngo TT, Dionne H, Abbott LF, Axel R, Tanimoto H, and Rubin GM (2014). The neuronal architecture of the mushroom body provides a logic for associative learning. eLife 3, e04577. 10.7554/eLife.04577. [PubMed: 25535793]

20. Mao Z, and Davis RL (2009). Eight different types of dopaminergic neurons innervate the Drosophila mushroom body neuropil: anatomical and physiological heterogeneity. Front. Neural Circuits 3, 5. 10.3389/neuro.04.005.2009. [PubMed: 19597562]

21. Heisenberg M (2003). Mushroom body memoir: from maps to models. Nat. Rev. Neurosci 4, 266–275. 10.1038/nrn1074. [PubMed: 12671643]

22. Tanaka NK, Tanimoto H, and Ito K (2008). Neuronal assemblies of the Drosophila mushroom body. J. Comp. Neurol 508, 711–755. 10.1002/cne.21692. [PubMed: 18395827]

23. Aso Y, and Rubin GM (2016). Dopaminergic neurons write and update memories with cell-type-specific rules. eLife 5, e16135. 10.7554/eLife.16135. [PubMed: 27441388]

24. Gerber B, König C, Fendt M, Andreatta M, Romanos M, Pauli P, and Yarali A (2019). Timing-dependent valence reversal: a principle of reinforcement processing and its possible implications. Curr. Opin. Behav. Sci 26, 114–120.

25. Gerber B, Yarali A, Diegelmann S, Wotjak CT, Pauli P, and Fendt M (2014). Pain-relief learning in flies, rats, and man: basic research and applied perspectives. Learn. Mem 21, 232–252. 10.1101/lm.032995.113. [PubMed: 24643725]

26. Tomchik SM, and Davis RL (2009). Dynamics of learning-related cAMP signaling and stimulus integration in the Drosophila olfactory pathway. Neuron 64, 510–521. 10.1016/j.neuron.2009.09.029. [PubMed: 19945393]

27. Berry JA, Phan A, and Davis RL (2018). Dopamine neurons mediate learning and forgetting through bidirectional modulation of a memory trace. Cell Rep 25. 651–662.e5. 10.1016/j.celrep.2018.09.051. [PubMed: 30332645]

28. Cohn R, Morantte I, and Ruta V (2015). Coordinated and compartmentalized neuromodulation shapes sensory processing in drosophila. Cell 163, 1742–1755. 10.1016/j.cell.2015.11.019. [PubMed: 26687359]

29. Handler A, Graham TGW, Cohn R, Morantte I, Siliciano AF, Zeng J, Li Y, and Ruta V (2019). Distinct dopamine receptor pathways underlie the temporal sensitivity of associative learning. Cell 178. 60–75.e19. 10.1016/j.cell.2019.05.040. [PubMed: 31230716]

30. Himmelreich S, Masuho I, Berry JA, MacMullen C, Skamangas NK, Martemyanov KA, and Davis RL (2017). Dopamine receptor DAMB signals via Gq to mediate forgetting in drosophila. Cell Rep 21, 2074–2081. 10.1016/j.celrep.2017.10.108. [PubMed: 29166600]

31. Galili DS, Lüdke A, Galizia CG, Szyszka P, and Tanimoto H (2011). Olfactory trace conditioning in Drosophila. J. Neurosci 31, 7240–7248. 10.1523/JNEUROSCI.6667-10.2011. [PubMed: 21593308]

32. Lüdke A, Raiser G, Nehrkorn J, Herz AVM, Galizia CG, and Szyszka P (2018). Calcium in kenyon cell somata as a substrate for an olfactory sensory memory in drosophila. Front. Cell. Neurosci 12, 128. 10.3389/fncel.2018.00128. [PubMed: 29867361]

33. Shuai Y, Hu Y, Qin H, Campbell RA, and Zhong Y (2011). Distinct molecular underpinnings of Drosophila olfactory trace conditioning. Proc. Natl. Acad. Sci. USA 108, 20201–20206. 10.1073/pnas.1107489109. [PubMed: 22123966]

34. Schwaerzel M, Monastirioti M, Scholz H, Friggi-Grelin F, Birman S, and Heisenberg M (2003). Dopamine and octopamine differentiate between aversive and appetitive olfactory memories in Drosophila. J. Neurosci 23, 10495–10502. [PubMed: 14627633]

35. Burke CJ, Huetteroth W, Owald D, Perisse E, Krashes MJ, Das G, Gohl D, Silies M, Certel S, and Waddell S (2012). Layered reward signalling through octopamine and dopamine in Drosophila. Nature 492, 433–437. 10.1038/nature11614. [PubMed: 23103875]

36. Liu C, Plaçais PY, Yamagata N, Pfeiffer BD, Aso Y, Friedrich AB, Siwanowicz I, Rubin GM, Preat T, and Tanimoto H (2012). A subset of dopamine neurons signals reward for odour memory in Drosophila. Nature 488, 512–516. 10.1038/nature11304. [PubMed: 22810589]

37. Kim YC, Lee HG, and Han KA (2007). D1 dopamine receptor dDA1 is required in the mushroom body neurons for aversive and appetitive learning in Drosophila. J. Neurosci 27, 7640–7647. 10.1523/JNEUROSCI.1167-07.2007. [PubMed: 17634358]

38. Qin H, Cressy M, Li W, Coravos JS, Izzi SA, and Dubnau J (2012). Gamma neurons mediate dopaminergic input during aversive olfactory memory formation in Drosophila. Curr. Biol 22, 608–614. 10.1016/j.cub.2012.02.014. [PubMed: 22425153]

39. Schroll C, Riemensperger T, Bucher D, Ehmer J, Völler T, Erbguth K, Gerber B, Hendel T, Nagel G, Buchner E, and Fiala A (2006). Light-induced activation of distinct modulatory neurons triggers appetitive or aversive learning in Drosophila larvae. Curr. Biol 16, 1741–1747. 10.1016/j.cub.2006.07.023. [PubMed: 16950113]

40. Claridge-Chang A, Roorda RD, Vrontou E, Sjulson L, Li H, Hirsh J, and Miesenböck G (2009). Writing memories with light-addressable reinforcement circuitry. Cell 139, 405–415. 10.1016/j.cell.2009.08.034. [PubMed: 19837039]

41. Waddell S, Armstrong JD, Kitamoto T, Kaiser K, and Quinn WG (2000). The amnesiac gene product is expressed in two neurons in the Drosophila brain that are critical for memory. Cell 103, 805–813. 10.1016/s0092-8674(00)00183-5. [PubMed: 11114336]

42. Keene AC, Krashes MJ, Leung B, Bernard JA, and Waddell S (2006). Drosophila dorsal paired medial neurons provide a general mechanism for memory consolidation. Curr. Biol 16, 1524–1530. 10.1016/j.cub.2006.06.022. [PubMed: 16890528]

43. Keene AC, Stratmann M, Keller A, Perrat PN, Vosshall LB, and Waddell S (2004). Diverse odor-conditioned memories require uniquely timed dorsal paired medial neuron output. Neuron 44, 521–533. 10.1016/j.neuron.2004.10.006. [PubMed: 15504331]

44. Yu D, Keene AC, Srivatsan A, Waddell S, and Davis RL (2005). Drosophila DPM neurons form a delayed and branch-specific memory trace after olfactory classical conditioning. Cell 123, 945–957. 10.1016/j.cell.2005.09.037. [PubMed: 16325586]

45. Krashes MJ, Keene AC, Leung B, Armstrong JD, and Waddell S (2007). Sequential use of mushroom body neuron subsets during Drosophila odor memory processing. Neuron 53, 103–115. 10.1016/j.neuron.2006.11.021. [PubMed: 17196534]

46. Wu CL, Shih MF, Lai JS, Yang HT, Turner GC, Chen L, and Chiang AS (2011). Heterotypic gap junctions between two neurons in the drosophila brain are critical for memory. Curr. Biol 21, 848–854. 10.1016/j.cub.2011.02.041. [PubMed: 21530256]

47. Ganguly A, Qi C, Bajaj J, and Lee D (2020). Serotonin receptor 5-HT7 in Drosophila mushroom body neurons mediates larval appetitive olfactory learning. Sci. Rep 10, 21267. 10.1038/s41598-020-77910-5. [PubMed: 33277559]
48. Johnson O, Becnel J, and Nichols CD (2011). Serotonin receptor activity is necessary for olfactory learning and memory in Drosophila melanogaster. Neuroscience 192, 372–381. 10.1016/j.neuroscience.2011.06.058. [PubMed: 21749913]
49. Lee PT, Lin HW, Chang YH, Fu TF, Dubnau J, Hirsh J, Lee T, and Chiang AS (2011). Serotonin-mushroom body circuit modulating the formation of anesthesia-resistant memory in Drosophila. Proc. Natl. Acad. Sci. USA 108, 13794–13799. 10.1073/pnas.1019483108. [PubMed: 21808003]
50. Haynes PR, Christmann BL, and Griffith LC (2015). A single pair of neurons links sleep to memory consolidation in Drosophila melanogaster. eLife 4, e03868. 10.7554/eLife.03868. [PubMed: 25564731]
51. Yamazaki D, Horiuchi J, Nakagami Y, Nagano S, Tamura T, and Saitoe M (2007). The Drosophila DCO mutation suppresses age-related memory impairment without affecting lifespan. Nat. Neurosci 10, 478–484. 10.1038/nn1863. [PubMed: 17322874]
52. Tonoki A, and Davis RL (2012). Aging impairs intermediate-term behavioral memory by disrupting the dorsal paired medial neuron memory trace. Proc. Natl. Acad. Sci. USA 109, 6319–6324. 10.1073/pnas.1118126109. [PubMed: 22474396]
53. Muria A, Musso PY, Durrieu M, Portugal FR, Ronsin B, Gordon MD, Jeanson R, and Isabel G (2021). Social facilitation of long-lasting memory is mediated by CO2 in Drosophila. Curr. Biol 31. 2065–2074.e5. 10.1016/j.cub.2021.02.044. [PubMed: 33740428]
54. Ries AS, Hermanns T, Poeck B, and Strauss R (2017). Serotonin modulates a depression-like state in Drosophila responsive to lithium treatment. Nat. Commun 8, 15738. 10.1038/ncomms15738. [PubMed: 28585544]
55. Sitaraman D, Zars M, Laferriere H, Chen YC, Sable-Smith A, Kitamoto T, Rottinghaus GE, and Zars T (2008). Serotonin is necessary for place memory in Drosophila. Proc. Natl. Acad. Sci. USA 105, 5579–5584. 10.1073/pnas.0710168105. [PubMed: 18385379]
56. Jing M, Li Y, Zeng J, Huang P, Skirzewski M, Kljakic O, Peng W, Qian T, Tan K, Zou J, et al. (2020). An optimized acetylcholine sensor for monitoring in vivo cholinergic activity. Nat. Methods 17, 1139–1146. 10.1038/s41592-020-0953-2. [PubMed: 32989318]
57. Jing M, Zhang P, Wang G, Feng J, Mesik L, Zeng J, Jiang H, Wang S, Looby JC, Guagliardo NA, et al. (2018). A genetically encoded fluorescent acetylcholine indicator for in vitro and in vivo studies. Nat. Biotechnol 36, 726–737. 10.1038/nbt.4184. [PubMed: 29985477]
58. Wan J, Peng W, Li X, Qian T, Song K, Zeng J, Deng F, Hao S, Feng J, Zhang P, et al. (2021). A genetically encoded sensor for measuring serotonin dynamics. Nat. Neurosci 24, 746–752. 10.1038/s41593-021-00823-7. [PubMed: 33821000]
59. Qian Y, Cao Y, Deng B, Yang G, Li J, Xu R, Zhang D, Huang J, and Rao Y (2017). Sleep homeostasis regulated by 5HT2B receptor in a small subset of neurons in the dorsal fan-shaped body of drosophila. eLife 6, e26519. 10.7554/eLife.26519. [PubMed: 28984573]
60. Yuan Q, Lin F, Zheng X, and Sehgal A (2005). Serotonin modulates circadian entrainment in Drosophila. Neuron 47, 115–127. 10.1016/j.neuron.2005.05.027. [PubMed: 15996552]
61. Hige T, Aso Y, Modi MN, Rubin GM, and Turner GC (2015). Heterosynaptic plasticity underlies aversive olfactory learning in drosophila. Neuron 88, 985–998. 10.1016/j.neuron.2015.11.003. [PubMed: 26637800]
62. Felsenberg J, Jacob PF, Walker T, Barnstedt O, Edmondson-Stait AJ, Pleijzier MW, Otto N, Schlegel P, Sharifi N, Perisse E, et al. (2018). Integration of parallel opposing memories underlies memory extinction. Cell 175. 709–722.e15. 10.1016/j.cell.2018.08.021. [PubMed: 30245010]
63. Perisse E, Owald D, Barnstedt O, Talbot CB, Huetteroth W, and Waddell S (2016). Aversive learning and appetitive motivation toggle feed-forward inhibition in the drosophila mushroom body. Neuron 90, 1086–1099. 10.1016/j.neuron.2016.04.034. [PubMed: 27210550]
64. Li F, Lindsey JW, Marin EC, Otto N, Dreher M, Dempsey G, Stark I, Bates AS, Pleijzier MW, Schlegel P, et al. (2020). The connectome of the adult Drosophila mushroom body provides insights into function. eLife 9, e62576. 10.7554/eLife.62576. [PubMed: 33315010]

65. Scheffer LK, Xu CS, Januszewski M, Lu Z, Takemura SY, Hayworth KJ, Huang GB, Shinomiya K, Maitlin-Shepard J, Berg S, et al. (2020). A connectome and analysis of the adult Drosophila central brain. eLife 9, e57443. 10.7554/eLife.57443. [PubMed: 32880371]
66. Eichler K, Li F, Litwin-Kumar A, Park Y, Andrade I, Schneider-Mizell CM, Saumweber T, Huser A, Eschbach C, Gerber B, et al. (2017). The complete connectome of a learning and memory centre in an insect brain. Nature 548, 175–182. 10.1038/nature23455. [PubMed: 28796202]
67. Takemura SY, Aso Y, Hige T, Wong A, Lu Z, Xu CS, Rivlin PK, Hess H, Zhao T, Parag T, et al. (2017). A connectome of a learning and memory center in the adult Drosophila brain. eLife 6, e26975. 10.7554/eLife.26975. [PubMed: 28718765]
68. Becnel J, Johnson O, Majeed ZR, Tran V, Yu B, Roth BL, Cooper RL, Kerut EK, and Nichols CD (2013). DREADDs in Drosophila: a pharmacogenetic approach for controlling behavior, neuronal signaling, and physiology in the fly. Cell Rep 4, 1049–1059. 10.1016/j.celrep.2013.08.003. [PubMed: 24012754]
69. Nagai Y, Miyakawa N, Takuwa H, Hori Y, Oyama K, Ji B, Takahashi M, Huang XP, Slocum ST, DiBerto JF, et al. (2020). Deschloroclozapine, a potent and selective chemogenetic actuator enables rapid neuronal and behavioral modulations in mice and monkeys. Nat. Neurosci 23, 1157–1167. 10.1038/s41593-020-0661-3. [PubMed: 32632286]
70. Tadres D, Shiozaki HM, Tastekin I, Stern DL, and Louis M (2022). An essential experimental control for functional connectivity mapping with optogenetics. Preprint at bioRxiv 10.1101/2022.05.26.493610.
71. Aso Y, Ray RP, Long X, Bushey D, Cichewicz K, Ngo TT, Sharp B, Christoforou C, Hu A, Lemire AL, et al. (2019). Nitric oxide acts as a cotransmitter in a subset of dopaminergic neurons to diversify memory dynamics. eLife 8, e49257. 10.7554/eLife.49257. [PubMed: 31724947]
72. Wu L, Dong A, Dong L, Wang SQ, and Li Y (2019). Paris, an optogenetic method for functionally mapping gap junctions. eLife 8, e43366. 10.7554/eLife.43366. [PubMed: 30638447]
73. Saudou F, Boschert U, Amlaiky N, Plassat JL, and Hen R (1992). A family of Drosophila serotonin receptors with distinct intracellular signalling properties and expression patterns. EMBO J 11, 7–17. [PubMed: 1310937]
74. Suzuki Y, Schenk JE, Tan H, and Gaudry Q (2020). A population of interneurons signals changes in the basal concentration of serotonin and mediates gain control in the drosophila antennal lobe. Curr. Biol 30. 1110–1118.e4. 10.1016/j.cub.2020.01.018. [PubMed: 32142699]
75. Lin AC, Bygrave AM, de Calignon A, Lee T, and Miesenböck G (2014). Sparse, decorrelated odor coding in the mushroom body enhances learned odor discrimination. Nat. Neurosci 17, 559–568. 10.1038/nn.3660. [PubMed: 24561998]
76. Inada K, Tsuchimoto Y, and Kazama H (2017). Origins of cell-type-specific olfactory processing in the drosophila mushroom body circuit. Neuron 95. 357–367.e4. 10.1016/j.neuron.2017.06.039. [PubMed: 28728024]
77. Amin H, Apostolopoulou AA, Suárez-Grimalt R, Vrontou E, and Lin AC (2020). Localized inhibition in the Drosophila mushroom body. eLife 9, e56954. 10.7554/eLife.56954. [PubMed: 32955437]
78. Wu Y, Ren Q, Li H, and Guo A (2012). The GABAergic anterior paired lateral neurons facilitate olfactory reversal learning in Drosophila. Learn. Mem 19, 478–486. 10.1101/lm.025726.112. [PubMed: 22988290]
79. Livingstone MS, Sziber PP, and Quinn WG (1984). Loss of calcium/ calmodulin responsiveness in adenylate cyclase of rutabaga, a Drosophila learning mutant. Cell 37, 205–215. [PubMed: 6327051]
80. Davis RL, Cherry J, Dauwalder B, Han PL, and Skoulakis E (1995). The cyclic AMP system and Drosophila learning. Mol. Cell. Biochem 149–150, 271–278. 10.1007/978-1-4615-2015-3_31.
81. Dudai Y, Sher B, Segal D, and Yovell Y (1985). Defective responsiveness of adenylate cyclase to forskolin in the Drosophila memory mutant rutabaga. J. Neurogenet 2, 365–380. 10.3109/01677068509101423. [PubMed: 3935769]
82. Levin LR, Han PL, Hwang PM, Feinstein PG, Davis RL, and Reed RR (1992). The Drosophila learning and memory gene rutabaga encodes a Ca2+/calmodulin-responsive adenylyl cyclase. Cell 68, 479–489. [PubMed: 1739965]

83. Gervasi N, Tchénio P, and Preat T (2010). PKA dynamics in a Drosophila learning center: coincidence detection by rutabaga adenylyl cyclase and spatial regulation by dunce phosphodiesterase. Neuron 65, 516–529. 10.1016/j.neuron.2010.01.014. [PubMed: 20188656]
84. Dudai Y, Jan YN, Byers D, Quinn WG, and Benzer S (1976). dunce, a mutant of Drosophila deficient in learning. Proc. Natl. Acad. Sci. USA 73, 1684–1688. 10.1073/pnas.73.5.1684. [PubMed: 818641]
85. Wang L, Wu C, Peng W, Zhou Z, Zeng J, Li X, Yang Y, Yu S, Zou Y, Huang M, et al. (2022). A high-performance genetically encoded fluorescent indicator for in vivo cAMP imaging. Nat. Commun 13, 5363. 10.1038/s41467-022-32994-7. [PubMed: 36097007]
86. Stahl A, Noyes NC, Boto T, Botero V, Broyles CN, Jing M, Zeng JZ, King LB, Li YL, Davis RL, et al. (2022). Associative learning drives longitudinally graded presynaptic plasticity of neurotransmitter release along axonal compartments. eLife 11, e76712. [PubMed: 35285796]
87. Aso Y, Sitaraman D, Ichinose T, Kaun KR, Vogt K, Belliart-Guérin G, Plaçais PY, Robie AA, Yamagata N, Schnaitmann C, et al. (2014). Mushroom body output neurons encode valence and guide memory-based action selection in Drosophila. eLife 3, e04580. 10.7554/eLife.04580. [PubMed: 25535794]
88. Felsenberg J, Barnstedt O, Cognigni P, Lin S, and Waddell S (2017). Re-evaluation of learned information in Drosophila. Nature 544, 240–244. 10.1038/nature21716. [PubMed: 28379939]
89. Chabaud MA, Isabel G, Kaiser L, and Preat T (2009). Social facilitation of long-lasting memory retrieval in Drosophila. Curr. Biol 19, 1654–1659. 10.1016/j.cub.2009.08.017. [PubMed: 19781943]
90. Sun YJ, Qiu R, Li XN, Cheng YX, Gao S, Kong FC, Liu L, and Zhu Y (2020). Social attraction in Drosophila is regulated by the mushroom body and serotonergic system. Nat. Commun 11, 5738. [PubMed: 33159087]
91. Okray Z, Jacob PF, Stern C, Desmond K, Otto N, Vargas-Gutierrez P, and Waddell S.J.b. (2022). Multisensory learning binds modality-specific neurons into a cross-modal memory engram. Preprint at bioRxiv 10.1101/2022.07.08.499174.
92. Scheunemann L, Plaçais PY, Dromard Y, Schwärzel M, and Preat T (2018). Dunce phosphodiesterase acts as a checkpoint for drosophila long-term memory in a pair of serotonergic neurons. Neuron 98. 350–365.e5. 10.1016/j.neuron.2018.03.032. [PubMed: 29673482]
93. Yarali A, Nehrkorn J, Tanimoto H, and Herz AV (2012). Event timing in associative learning: from biochemical reaction dynamics to behavioural observations. PLoS One 7, e32885. 10.1371/journal.pone.0032885. [PubMed: 22493657]
94. Kandel ER (2001). The molecular biology of memory storage: a dialogue between genes and synapses. Science 294, 1030–1038. 10.1126/science.1067020. [PubMed: 11691980]
95. Kandel ER, and Schwartz JH (1982). Molecular biology of learning: modulation of transmitter release. Science 218, 433–443. 10.1126/science.6289442. [PubMed: 6289442]
96. Zhang Y, Lu H, and Bargmann CI (2005). Pathogenic bacteria induce aversive olfactory learning in Caenorhabditis elegans. Nature 438, 179–184. 10.1038/nature04216. [PubMed: 16281027]
97. Liu Z, Lin R, and Luo M (2020). Reward contributions to serotonergic functions. Annu. Rev. Neurosci 43, 141–162. 10.1146/annurev-neuro-093019-112252. [PubMed: 32640931]
98. Liu Z, Zhou J, Li Y, Hu F, Lu Y, Ma M, Feng Q, Zhang JE, Wang D, Zeng J, et al. (2014). Dorsal raphe neurons signal reward through 5-HT and glutamate. Neuron 81, 1360–1374. 10.1016/j.neuron.2014.02.010. [PubMed: 24656254]
99. Ren J, Friedmann D, Xiong J, Liu CD, Ferguson BR, Weerakkody T, DeLoach KE, Ran C, Pun A, Sun Y, et al. (2018). Anatomically defined and functionally distinct dorsal raphe serotonin sub-systems. Cell 175. 472–487.e20. 10.1016/j.cell.2018.07.043. [PubMed: 30146164]
100. Buhot MC, Martin S, and Segu L (2000). Role of serotonin in memory impairment. Ann. Med 32, 210–221. 10.3109/07853890008998828. [PubMed: 10821328]
101. Fonseca MS, Murakami M, and Mainen ZF (2015). Activation of dorsal raphe serotonergic neurons promotes waiting but is not reinforcing. Curr. Biol 25, 306–315. 10.1016/j.cub.2014.12.002. [PubMed: 25601545]

102. Lottem E, Banerjee D, Vertechi P, Sarra D, Lohuis MO, and Mainen ZF (2018). Activation of serotonin neurons promotes active persistence in a probabilistic foraging task. Nat. Commun 9, 1000. 10.1038/s41467-018-03438-y. [PubMed: 29520000]

103. Miyazaki K, Miyazaki KW, and Doya K (2011). Activation of dorsal raphe serotonin neurons underlies waiting for delayed rewards. J. Neurosci 31, 469–479. 10.1523/JNEUROSCI.3714-10.2011. [PubMed: 21228157]

104. Miyazaki KW, Miyazaki K, and Doya K (2011). Activation of the central serotonergic system in response to delayed but not omitted rewards. Eur. J. Neurosci 33, 153–160. 10.1111/j.1460-9568.2010.07480.x. [PubMed: 21070390]

105. Miyazaki KW, Miyazaki K, and Doya K (2012). Activation of dorsal raphe serotonin neurons is necessary for waiting for delayed rewards. J. Neurosci 32, 10451–10457. 10.1523/JNEUROSCI.0915-12.2012. [PubMed: 22855794]

106. Miyazaki KW, Miyazaki K, Tanaka KF, Yamanaka A, Takahashi A, Tabuchi S, and Doya K (2014). Optogenetic activation of dorsal raphe serotonin neurons enhances patience for future rewards. Curr. Biol 24, 2033–2040. 10.1016/j.cub.2014.07.041. [PubMed: 25155504]

107. Miyazaki K, Miyazaki KW, Yamanaka A, Tokuda T, Tanaka KF, and Doya K (2018). Reward probability and timing uncertainty alter the effect of dorsal raphe serotonin neurons on patience. Nat. Commun 9, 2048. 10.1038/s41467-018-04496-y. [PubMed: 29858574]

108. Tanaka SC, Shishida K, Schweighofer N, Okamoto Y, Yamawaki S, and Doya K (2009). Serotonin affects association of aversive outcomes to past actions. J. Neurosci 29, 15669–15674. 10.1523/JNEUROSCI.2799-09.2009. [PubMed: 20016081]

109. He K, Huertas M, Hong SZ, Tie X, Hell JW, Shouval H, and Kirkwood A (2015). Distinct eligibility traces for LTP and LTD in cortical synapses. Neuron 88, 528–538. 10.1016/j.neuron.2015.09.037. [PubMed: 26593091]

110. Hong SZ, Mesik L, Grossman CD, Cohen JY, Lee B, Severin D, Lee HK, Hell JW, and Kirkwood A (2022). Norepinephrine potentiates and serotonin depresses visual cortical responses by transforming eligibility traces. Nat. Commun 13, 3202. 10.1038/s41467-022-30827-1. [PubMed: 35680879]

111. Yagishita S, Hayashi-Takagi A, Ellis-Davies GC, Urakubo H, Ishii S, and Kasai H (2014). A critical time window for dopamine actions on the structural plasticity of dendritic spines. Science 345, 1616–1620. 10.1126/science.1255514. [PubMed: 25258080]

112. Yamaguchi K, Maeda Y, Sawada T, Iino Y, Tajiri M, Nakazato R, Ishii S, Kasai H, and Yagishita S (2022). A behavioural correlate of the synaptic eligibility trace in the nucleus accumbens. Sci. Rep 12, 1921. 10.1038/s41598-022-05637-6. [PubMed: 35121769]

113. Brzosko Z, Schultz W, and Paulsen O (2015). Retroactive modulation of spike timing-dependent plasticity by dopamine. eLife 4, e09685. 10.7554/eLife.09685. [PubMed: 26516682]

114. Brzosko Z, Mierau SB, and Paulsen O (2019). Neuromodulation of spike-timing-dependent plasticity: past, present, and future. Neuron 103, 563–581. 10.1016/j.neuron.2019.05.041. [PubMed: 31437453]

115. Gerstner W, Lehmann M, Liakoni V, Corneil D, and Brea J (2018). Eligibility traces and plasticity on behavioral time scales: experimental support of NeoHebbian three-factor learning rules. Front. Neural Circuits 12, 53. 10.3389/fncir.2018.00053. [PubMed: 30108488]

116. Cassenaer S, and Laurent G (2007). Hebbian STDP in mushroom bodies facilitates the synchronous flow of olfactory information in locusts. Nature 448, 709–713. 10.1038/nature05973. [PubMed: 17581587]

117. Doya K (2002). Metalearning and neuromodulation. Neural Netw 15, 495–506. 10.1016/s0893-6080(02)00044-8. [PubMed: 12371507]

118. Doya K, Miyazaki KW, and Miyazaki K (2021). Serotonergic modulation of cognitive computations 38. 116–123.

## Highlights

- 5-HT regulates the coincidence time window of Drosophila olfactory learning
- GRAB sensor reveals compartmental 5-HT release in the mushroom body
- The serotonergic DPM neuron provides inhibitory feedback to KCs
- 5-HT levels gate the intrinsic coincidence time windows of distinct MB compartments

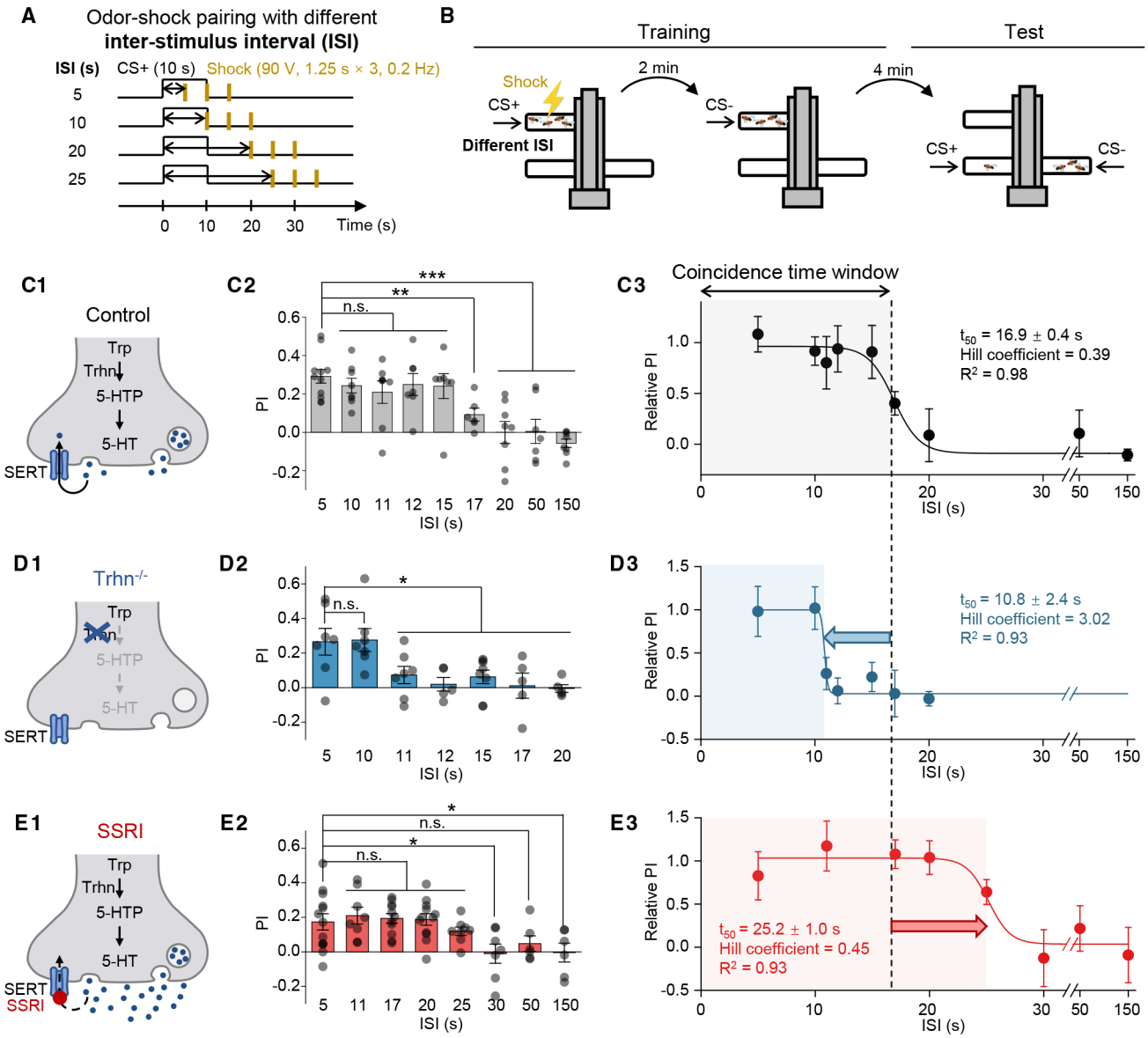


**Figure 1. 5-HT bi-directionally regulates the coincidence time window of olfactory learning**

(A and B) Schematics depicting the protocol for odor-shock pairing with varying ISIs (A) and the T-maze assay for measuring the olfactory memory (B).

(C–E) (C1–E1) Schematics depicting the control flies, Trhn$^{-/-}$ flies, and the SSRI-fed flies (10 mM fluoxetine). (C2–E2) Summary of the PI measured with the indicated ISI; n = 5–11 for each group. (C3–E3) The relative PI-ISI profile fitted with a sigmoid function; the $t_{50}$ ± standard error, Hill coefficient, and $R^2$ are shown. The coincidence time window is defined as the $t_{50}$ and indicated by the shaded area. The dashed vertical line at 16.9 s represents the coincidence time window of control flies.

In this and subsequent figures, all summary data are presented as the mean ± SEM, superimposed with individual data.

*p < 0.05; **p < 0.01; ***p < 0.001; and n.s., not significant (unpaired Student's t test).

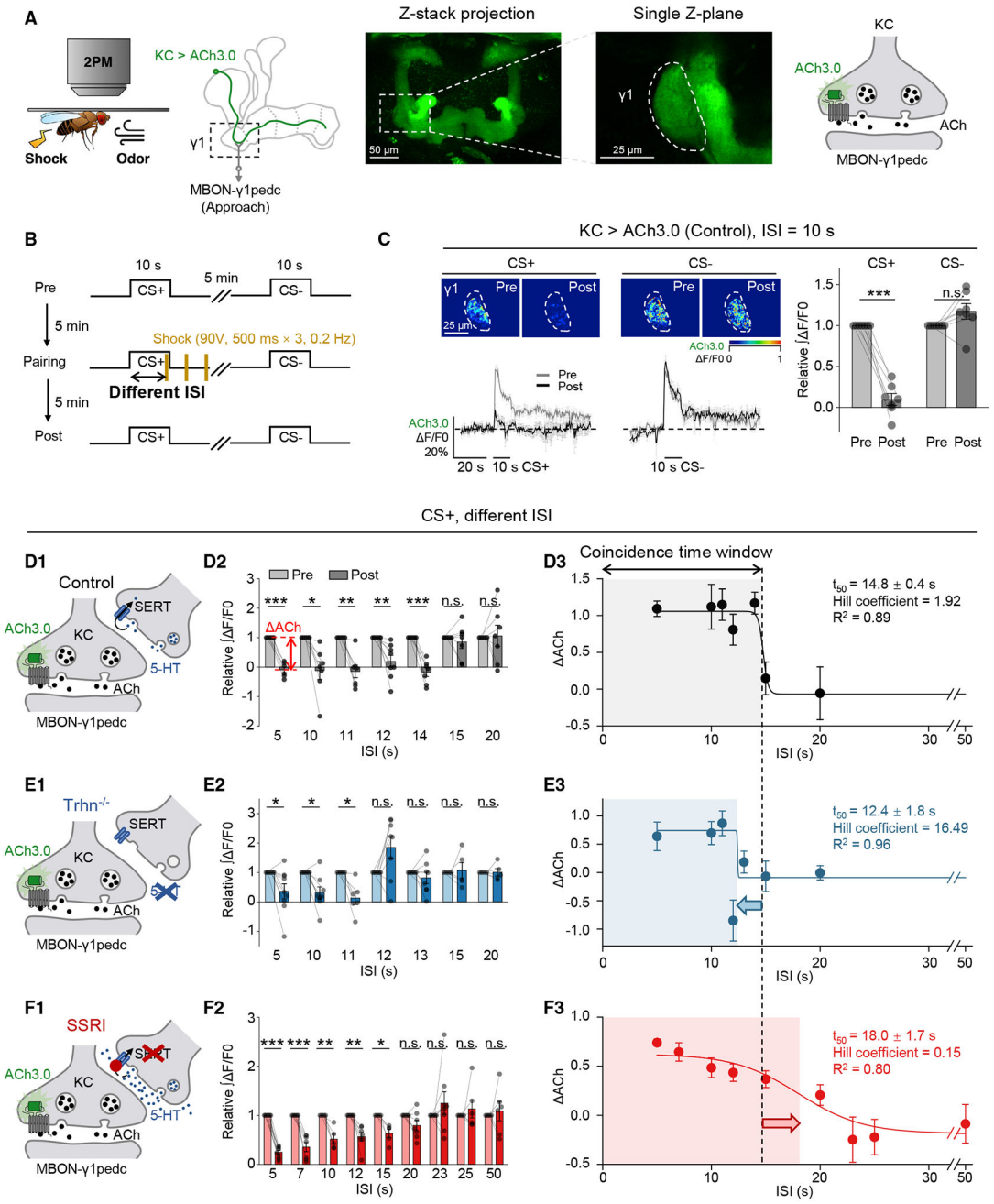


**Figure 2. 5-HT regulates the coincidence time window for inducing synaptic depression**

(A and B) Schematics depicting the *in vivo* two-photon imaging setup, fluorescence images (A), and the experimental protocol (B), in which odor-induced ACh signals in the γ1 compartment pre- and post-pairing were measured with ACh3.0 expressed in KCs. (C) Representative pseudocolor images (top left), average (± SEM) traces (bottom left), and summary of the relative change (right) of odor-induced ACh signals pre- and post-pairing. (D–F) (D1–F1) Schematics depicting ACh3.0 imaging experiments in the control flies, Trhn$^{-/-}$ flies, and SSRI-fed flies (10 mM fluoxetine). (D2–F2) Summary of the relative change of the integrated ACh3.0 fluorescence in response to CS+ with the indicated

ISI; n = 5–9 flies/group. ΔACh indicates the difference between pre- and post-responses. (D3–F3) The ΔACh-ISI profile fitted with a sigmoid function; the $t_{50}$ ± standard error, Hill coefficient, and $R^2$ are shown. The coincidence time window for inducing synaptic depression is defined as the $t_{50}$ and indicated by the shaded area. The dashed vertical line at 14.8 s represents the coincidence time window of control flies.
*p < 0.05; **p < 0.01; ***p < 0.001; and n.s., not significant (paired Student's t test).
See also Figures S1 and S2.

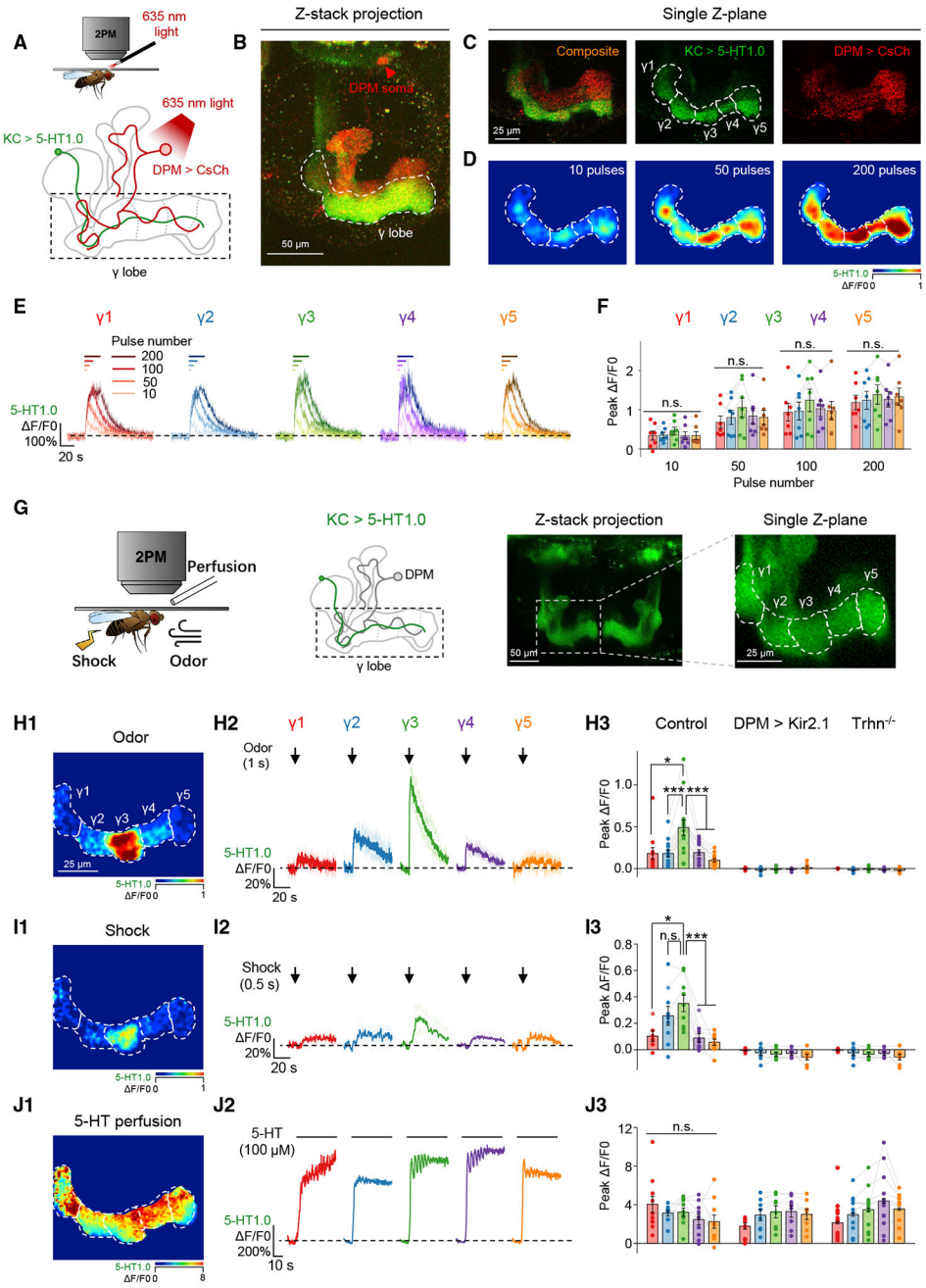


**Figure 3. The GRAB$_{5\text{-HT1.0}}$ sensor reveals physiological stimuli-evoked heterogeneous 5-HT signals from the DPM neuron**

(A–F) Optogenetically activating the DPM neuron induces homogeneous release of 5-HT in the γ lobe. Shown are schematics (A) and fluorescence images (B and C) depicting the *in vivo* imaging setup, in which the CsCh (short for CsChrimson)-expressing DPM neuron was activated with light pulses (1 ms/pulse, 635 nm, 10 Hz), and 5-HT was measured using 5-HT1.0 expressed in the KCs. Also shown are representative pseudocolor images (D), average traces (E), and summary (F) of the change in 5-HT1.0 fluorescence in response to the indicated number of light pulses; n = 7 flies/group. The nAChR antagonist Meca (100 μM) was applied to avoid indirect activation.

(G–J) Physiological stimuli induce heterogeneous 5-HT signals in the γ lobe. Shown are schematics and fluorescence images (G) depicting the *in vivo* imaging setup, in which 5-HT was measured using 5-HT1.0 expressed in the KCs. Also shown are pseudocolor images (H1–J1), average and individual traces (H2–J2), and summary (H3–J3) of the change in 5-HT1.0 fluorescence in response to odor (1 s), electric shock (0.5 s, 90 V), and 5-HT perfusion (100 μM) in control flies, DPM > Kir2.1 flies, and $Trhn^{-/-}$ flies; n = 6–14 flies/group.

*p < 0.05; ***p < 0.001; and n.s., not significant (paired or unpaired Student's t test).

See also Figures S1 and S3.

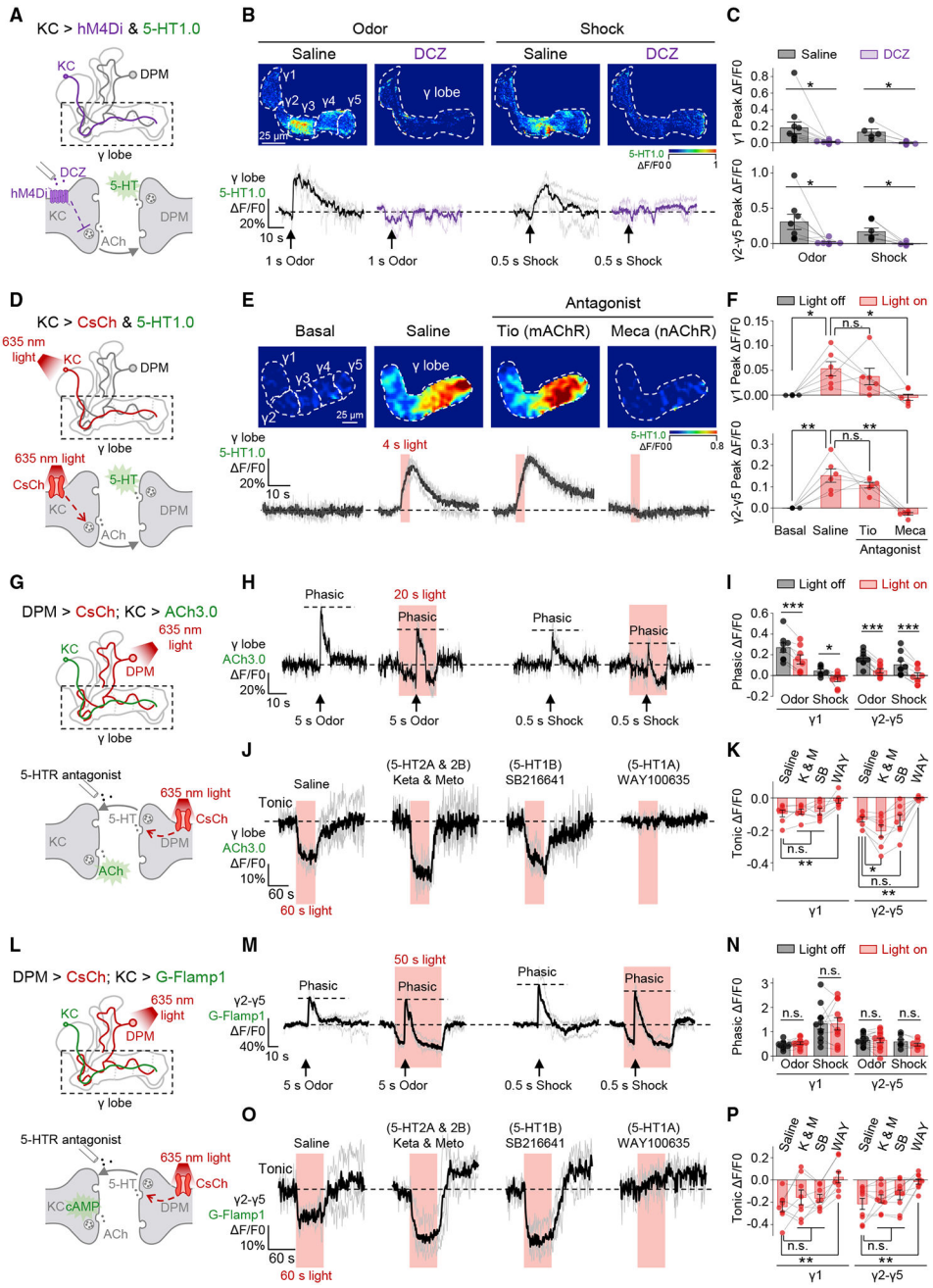


**Figure 4. 5-HT release from the DPM neuron is activated by ACh from KCs, and the 5-HT signal provides inhibitory feedback on KCs**

(A–C) Silencing KCs abolishes stimuli-evoked 5-HT release in the γ lobe. Shown are schematics (A) depicting the *in vivo* imaging setup in which hM4Di-expressing KCs were silenced by DCZ (30 nM), and 5-HT was measured using 5-HT1.0 expressed in KCs. Also shown are representative pseudocolor images (B, top), average and individual traces (B, bottom), and summary (C) of the change in 5-HT1.0 fluorescence in response to odor (1 s) or electric shock (0.5 s, 90 V) in flies with or without DCZ; n = 5–11 flies/group. In each fly, the experiment was divided into saline and DCZ sessions, and in each session, the odor and/or shock stimuli were applied for 1–3 trials, in random order.

(D–F) Activating KCs induces 5-HT release in the γ lobe. Shown are schematics (D) depicting the *in vivo* imaging setup in which CsChrimson-expressing KCs were activated by light pulses (1 ms/pulse, 635 nm, 10 Hz), and 5-HT was measured using 5-HT1.0 expressed in KCs. Also shown are representative pseudocolor images (E, top), average and individual traces (E, bottom), and summary (F) of the change in 5-HT1.0 fluorescence in response to optogenetic stimulation in saline or in the presence of either the mAChR antagonist Tio (100 μM) or the nAChR antagonist Meca (100 μM); n = 6 flies/group. For each fly, the experiment was divided into three sessions, and in each session the light was applied for 3 trials.

(G–K) Activating the DPM neuron inhibits both stimuli-evoked (phasic) and spontaneous (tonic) ACh release in the γ lobe. Shown are schematics (G) depicting the *in vivo* imaging setup in which the CsChrimson-expressing DPM neuron was activated by light pulses (5 ms/pulse, 635 nm, 4 Hz), and ACh was measured using ACh3.0 expressed in KCs. Also shown are average and individual traces (H and J), and summary (I and K) of the change in ACh3.0 fluorescence in response to odor (5-s application) and electric shock (0.5 s, 90 V) with or without light stimulation, or to 60-s light stimulation with or without 5-HT receptors' antagonists (20 μM); n = 7–9 flies/group. When measuring phasic signals, a fly received 2–8 pairs of odor and/or shock stimuli, and in each pair the light-on and light-off trials were performed in random order. When measuring tonic signals, each fly was tested in 4 sessions, and in each session the light were applied for 3 trials. The gap junction blocker CBX (100 μM) was present throughout the experiment.

(L–P) Activating the DPM neuron selectively inhibits spontaneous (tonic) but does not influence stimuli-evoked (phasic) cAMP dynamics in the γ lobe. Shown are similar to (G)–(K) except that cAMP was measured using G-Flamp1 expressed in KCs; n = 8–15 flies/group.

*p < 0.05; **p < 0.01; ***p < 0.001; and n.s., not significant (paired Student's t test).

See also Figures S3–S6.

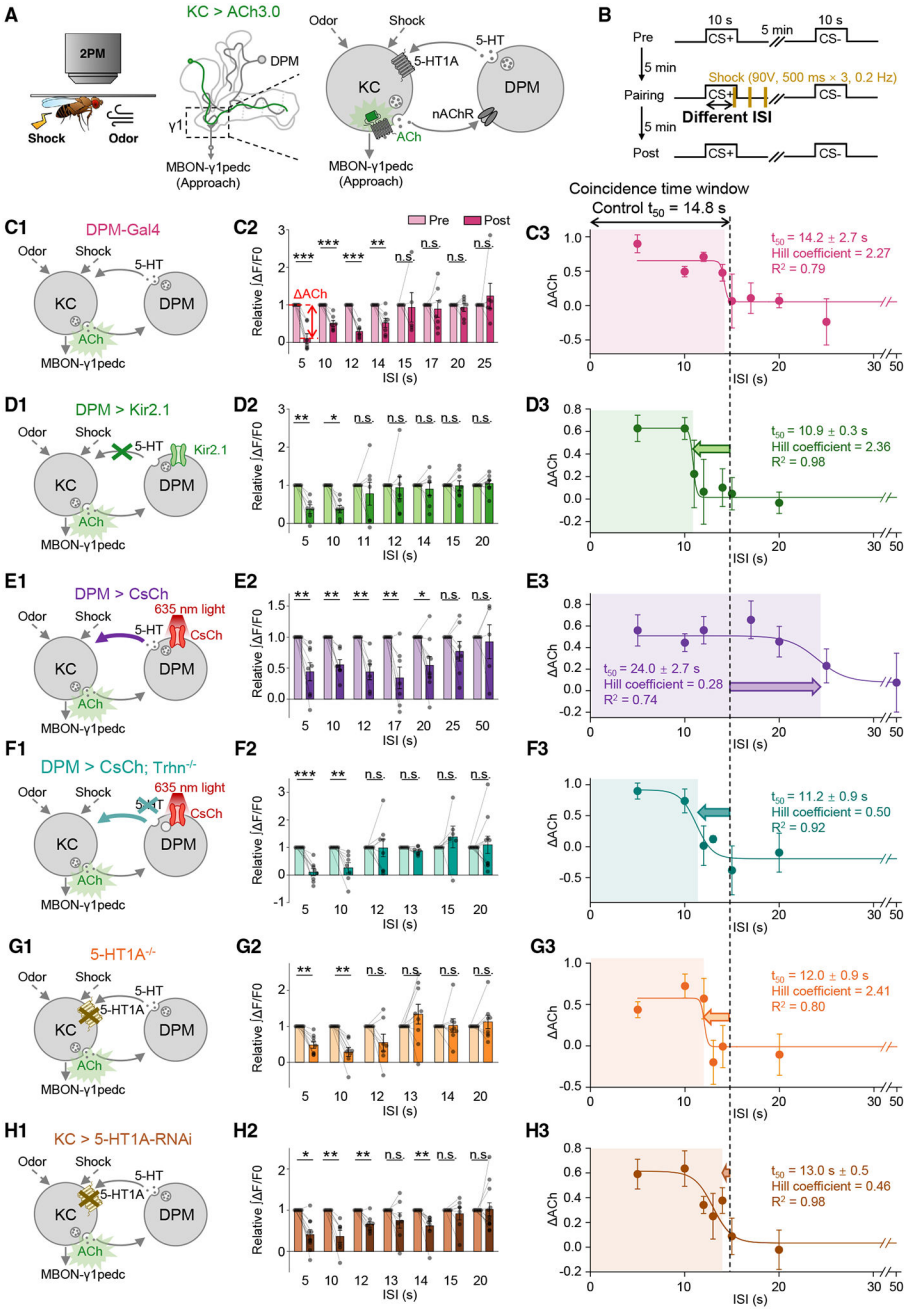


**Figure 5. 5-HT signal from the DPM neuron bi-directionally modulates the coincidence time window for synaptic depression in the γ1 compartment**

(A and B) Schematics depicting the *in vivo* imaging setup (A, left), the inhibitory feedback loop of the DPM neuron and KCs (A, right), and the experimental protocol (B).

(C–H) (C1–H1) Schematics depicting the measurement of synaptic depression in the γ1 compartment, using ACh3.0 expressed in KCs, with the indicated genetic perturbations affecting the serotonergic DPM-to-KCs signaling. In (E), the CsChrimson-expressing DPM neuron was activated by continuous 635-nm light from the start of the odor application to 4.5 s after the last electric shock being applied. (F) was similar to (E), except that $Trhn^{-/-}$ flies were used. (C2–H2) Summary of the relative change of the integrated ACh3.0

fluorescence in response to the CS+ in pre- and post-pairing sessions with the indicated ISI. ΔACh indicates the difference between pre- and post-responses; n = 5–10 flies/group. (C3–H3) The ΔACh-ISI profile was fitted to a sigmoid function; the $t_{50}$ ± standard error, Hill coefficient, and $R^2$ are shown. The dashed vertical line at 14.8 s represents the coincidence time window of synaptic depression in control flies.

*p < 0.05; **p < 0.01; ***p < 0.001; and n.s., not significant (paired Student's t test).

See also Figure S2.

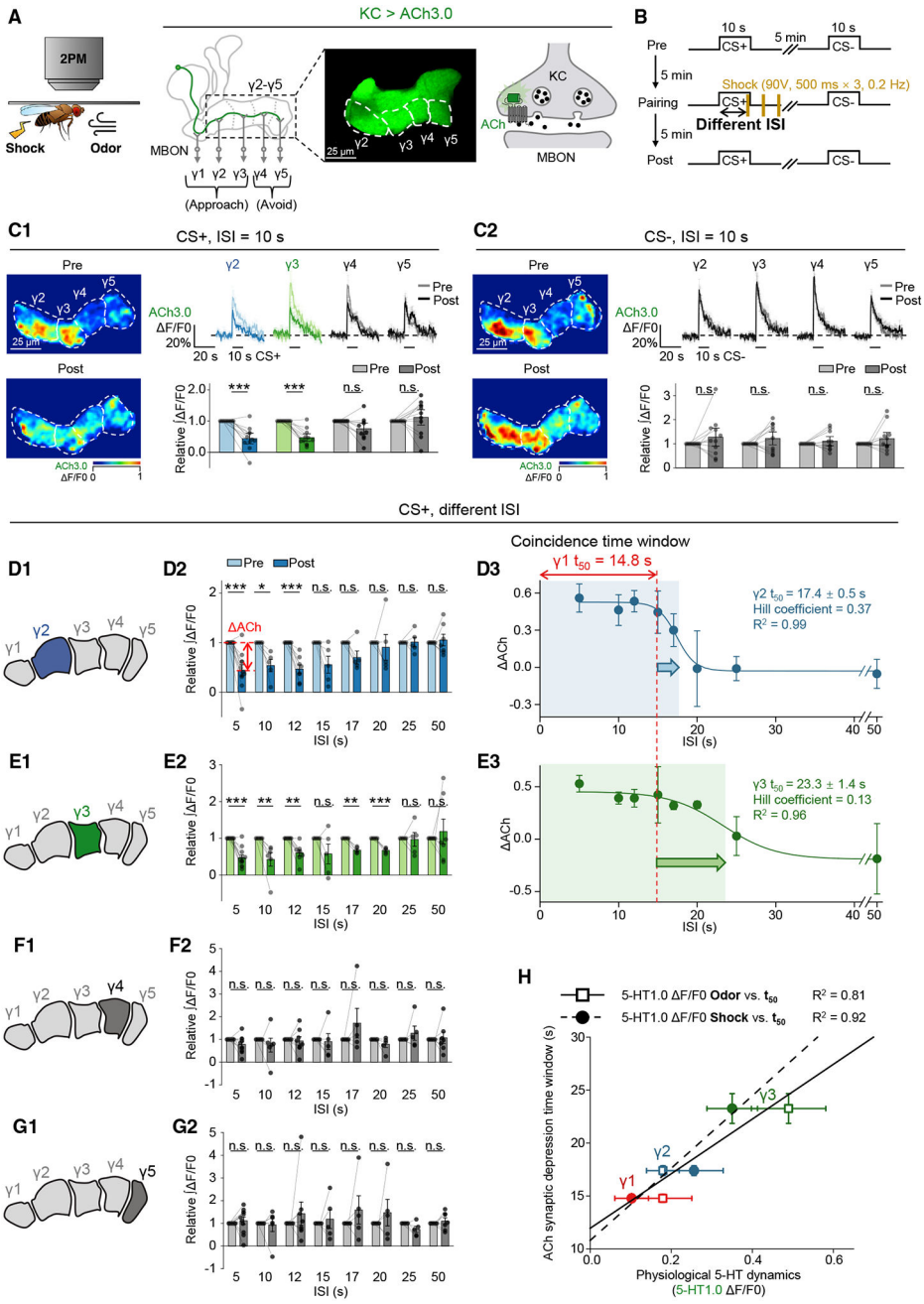


**Figure 6. Heterogeneous 5-HT signals gate the lengths of coincidence time windows for inducing synaptic depression in the γ1–γ3 compartments**

(A and B) Schematics depicting the *in vivo* imaging setup (A) and experimental protocol (B) for measuring changes in synaptic plasticity in the γ2–γ5 compartments, using ACh3.0 expressed in KCs.

(C) Flies were trained with odor-shock pairing with 10-s ISI, and changes in ACh3.0 fluorescence were compared between the pre- and post-pairing sessions, in response to the CS+ (C1) and CS− (C2). Shown are representative pseudocolor images (left), average (± SEM) traces (top right), and the summary (bottom right) of the ACh3.0 fluorescence; n = 11 flies/group.

(D–G) (D1–G1) Schematics depicting the measurement of synaptic depression in different γ lobe compartments, using ACh3.0 expressed in KCs. (D2–G2) Summary of the relative change of the integrated ACh3.0 fluorescence in response to the CS+ in pre- and post-pairing sessions with the indicated ISI. ΔACh indicates the difference between pre- and post-responses; n = 4–10 flies/group. (D3–E3) The ΔACh-ISI profile was fitted to a sigmoid function; the $t_{50}$ ± standard error, Hill coefficient, and $R^2$ are shown. The dashed vertical line at 14.8 s represents the coincidence time window measured for the γ1 compartment.
(H) Correlation analysis of coincidence time windows (y axis: $t_{50}$ ± standard error) for inducing synaptic depression and the odor- or shock-evoked 5-HT dynamics (x axis: ΔF/F0 ± standard error) in γ1–γ3 compartments. Each set of data was fit to a linear function, and the $R^2$ is shown.
*p < 0.05; **p < 0.01; ***p < 0.001; and n.s., not significant (paired Student's t test).
See also Figure S2.

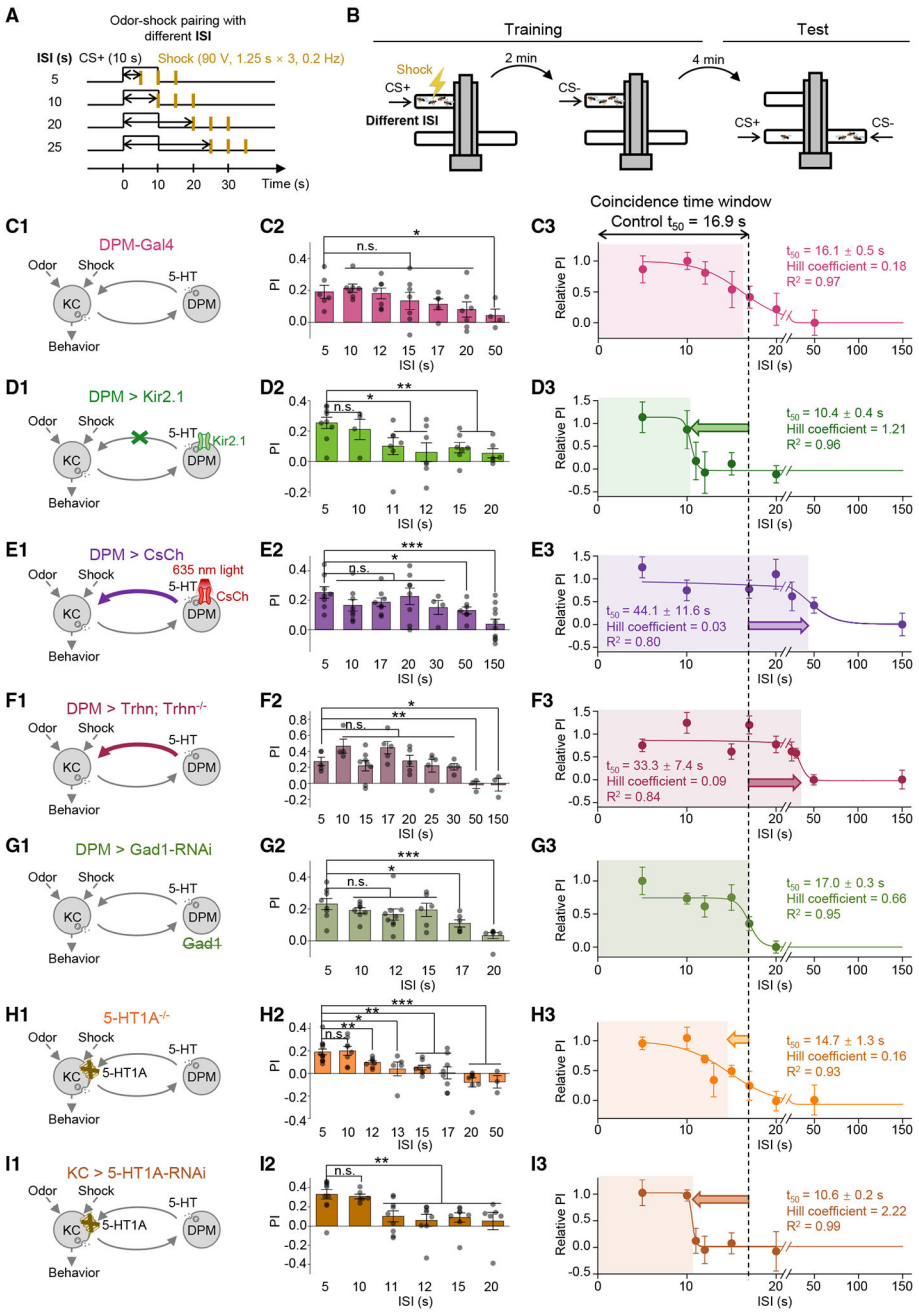


**Figure 7. 5-HT from the DPM neuron bi-directionally modulates the coincidence time window of olfactory learning**

(A and B) Schematics depicting the protocol for odor-shock pairing with varying ISIs (A) and the T-maze assay for measuring the olfactory memory (B).

(C–I) (C1–I1): schematics depicting the genetic perturbations affecting the serotonergic DPM-to-KC signaling. In (E), the CsChrimson-expressing DPM neuron was activated by continuous 635-nm light applied from the start of the odorant application to 3.75 s after the last electric shock being applied. (C2–I2) Summary of the PI measured with the indicated ISI; n = 3–10 for each group. (C3–I3): the relative PI-ISI profile was fitted to a sigmoid function; the $t_{50}$ ± standard error, Hill coefficient, and $R^2$ are shown. The dashed vertical line

at 16.9 s represents the coincidence time window of olfactory learning measured in control flies.

*p < 0.05; **p < 0.01; ***p < 0.001; and n.s., not significant (unpaired Student's t test). See also Figure S3.

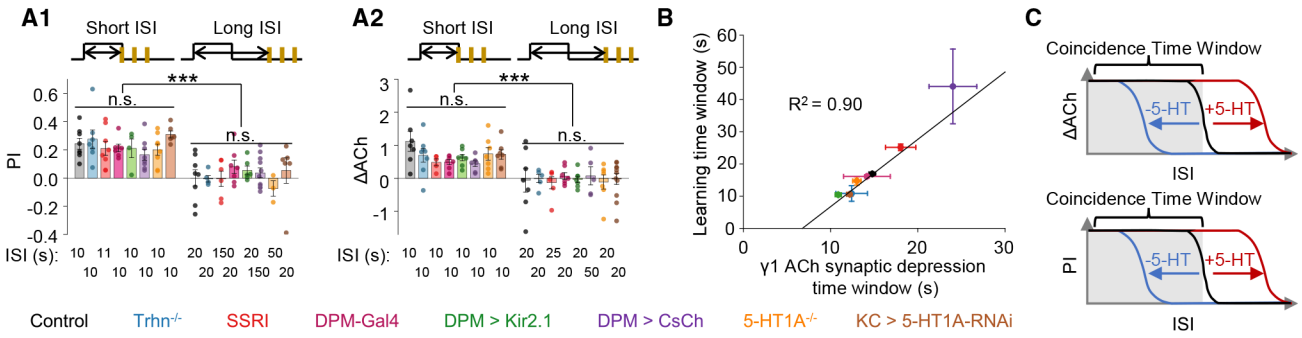


**Figure 8. 5-HT from the DPM neuron serves as a specialized regulator of the coincidence time window**

(A) Summary of the PI (A1) and ΔACh (A2) measured in the indicated flies with short and long ISIs; n = 3–10 for each group.

(B) Correlation analysis of coincidence time windows (y axis: $t_{50}$ ± standard error) measured in olfactory learning and that for inducing synaptic depression in the γ1 compartment (x axis: $t_{50}$ ± standard error) of the indicated flies. The data were fit to a linear function, and the $R^2$ is shown.

(C) Schematics depicting the working model that the increase or decrease of 5-HT signal from the DPM neuron prolongs or shortens, respectively, the coincidence time window for inducing synaptic depression of ACh release from KCs, and it ultimately affects the olfactory learning behavior.

***p < 0.001 and n.s., not significant (unpaired Student's t test).

See also Figures S7 and S8

## KEY RESOURCES TABLE

| REAGENT or RESOURCE | SOURCE | IDENTIFIER |
|---|---|---|
| Antibodies | | |
| Anti-GFP | Abcam | Cat #13970; RRID: AB_300798 |
| Anti-mCherry | Abcam | Cat #ab167453; RRID: AB_2571870 |
| Anti-nc82 | DSHB | Cat #2314866; RRID: AB_2314866 |
| Alexa Flour 488 anti-chicken | Molecular Probes | Cat #A-11039; RRID: AB_142924 |
| Alexa Flour 555 anti-rabbit | AAT Bioquest | Cat #16690 |
| Alexa Flour 647 anti-mouse | AAT Bioquest | Cat #16562 |
| Chemicals, peptides, and recombinant proteins | | |
| Dopamine (DA) | Sigma-Aldrich | Cat #H8502 |
| Acetylcholine (ACh) | Solarbio | Cat #G8320 |
| Mecamylamine (Meca) | Sigma-Aldrich | Cat #M9020 |
| Tiotropium (Tio) | Dexinjia Bio &Tech | N/A |
| All-trans-retinal | Sigma-Aldrich | Cat #R2500 |
| 5-hydroxytryptamine (5-HT) | Tocris | Cat #3547 |
| Deschloroclozapine (DCZ) | MedChemExpress | Cat #HY-42110 |
| Octopamine (OA) | Tocris | Cat #2242 |
| Glutamate (Glu) | Sigma-Aldrich | Cat #V900408 |
| γ-aminobutyric acid (GABA) | Tocris | Cat #0344 |
| Ketanserin (Keta) | Aladdin | Cat #K107929 |
| Metoclopramide (Meto) | APExBIO | Cat #A3599 |
| SB216641 (SB) | APExBIO | Cat #B6653 |
| WAY-100635 (WAY) | Macklin | Cat #W855249 |
| Mineral oil | Sigma-Aldrich | Cat #69794 |
| 3-Octanol (OCT) | Sigma-Aldrich | Cat #218405 |
| 4-Methylcyclohexanol (MCH) | Sigma-Aldrich | Cat #153095 |
| Isoamyl acetate (IA) | Sigma-Aldrich | Cat #306967 |
| Fluoroshield | Sigma-Aldrich | Cat #F6182 |
| Fluoxetine | Sigma-Aldrich | Cat #F132 |
| Carbenoxolone (CBX) | Sigma-Aldrich | Cat #C4790 |
| CGP54626 (CGP) | Tocris | Cat #1088 |
| Picrotoxin (PTX) | Tocris | Cat #1128 |
| Experimental models: Organisms/strains | | |
| Canton-S (W1118) | Yi Rao, Peking University | N/A |
| Trh01 ($Trhn^{-/-}$) | Qian et al.[59] | N/A |
| 5-HT1A$^{Gal4}$ (5-$HT1A^{-/-}$) | Qian et al.[59] | N/A |
| LexAop2-ACh3.0 (chr2) | Jing et al.[56] | BDSC: 86551 |
| LexAop2-ACh3.0 (chr3) | Jing et al.[56] | BDSC: 86552 |
| UAS-5-HT1.0 (chr2) | Wan et al.[58] | BDSC: 90874 |
| LexAop2-5-HT1.0 (chr2) | Wan et al.[58] | BDSC: 90876 |

| REAGENT or RESOURCE | SOURCE | IDENTIFIER |
|---|---|---|
| LexAop2-5-HT1.0 (chr3) | Wan et al.[58] | BDSC: 90877 |
| MB247-LexA | Yi Zhong, Tsinghua University | N/A |
| R13F02-Gal4 | Yi Rao, Peking University | BDSC: 48571 |
| R13F02-LexA | Yi Rao, Peking University | BDSC: 52460 |
| 30y-Gal4 | Yi Rao, Peking University | BDSC: 30818 |
| VT064246-Gal4 | Yi Rao, Peking University | VDRC: 204311 |
| UAS-CsChrimson-mCherry | Chuan Zhou, Institute of Zoology, CAS | BDSC: 82181 |
| UAS-Kir2.1 | Chuan Zhou, Institute of Zoology, CAS | N/A |
| UAS-hM4Di | Donggen Luo, Peking University | N/A |
| LexAop2-G-Flamp1 (chr2) | Wang et al.[85] | N/A |
| UAS-5HT1A-RNAi | Jianquan Ni, TsingHuafly center | THU1216 |
| UAS-Gad1-RNAi | Yan Li, Institute of Biophysics, CAS | BDSC: 28079 |
| UAS-Trhn | Bloomington Drosophila Stock Center | BDSC: 27638 |
| R12G04-LexA | Bloomington Drosophila Stock Center | BDSC: 52448 |
| LexAop2-GCaMP6s (chr3) | Bloomington Drosophila Stock Center | BDSC: 44274 |
| UAS-GCaMP5 (chr2) | Bloomington Drosophila Stock Center | BDSC: 42037 |
| C316-Gal4 | Bloomington Drosophila Stock Center | BDSC: 30830 |
| L0111-lexA | Yi Rao, Peking University | N/A |
| LexAop2-CsChrimson.tdTomato | Bloomington Drosophila Stock Center | BDSC: 82183 |
| GH146-Gal4 | Bloomington Drosophila Stock Center | BDSC: 30026 |
| UAS-GCaMP5 (chr3) | Bloomington Drosophila Stock Center | BDSC: 42038 |
| Software and algorithms | | |
| Origin2019 | OriginLab | https://imagej.nih.gov/ij/; RRID: SCR_003070 |
| ImageJ | NIH | https://imagej.nih.gov/ij/; RRID: SCR_003070 |
| Arduino UNO | Arduino.cc | https://www.arduino.cc/en/Guide/ArduinoUno; RRID:SCR_017284 |
| Matlab R2019b | MathWorks | https://www.mathworks.com/; RRID:SCR_001622 |